Geosphere

Early Miocene volcanic activity and paleoenvironment conditions recorded in tephra layers of the AND-2A core (southern McMurdo Sound, Antarctica).

--Manuscript Draft--

Manuscript Number:	GS754R2
Full Title:	Early Miocene volcanic activity and paleoenvironment conditions recorded in tephra layers of the AND-2A core (southern McMurdo Sound, Antarctica).
Short Title:	
Article Type:	Research Paper
Keywords:	Antarctica, volcaniclastic sediments, paleoenvironment, Mt. Morning, Victoria Land Basin
Corresponding Author:	Alessio Di Roberto, Ph.D. Istituto Nazionale di Geofisica e Vulcanologia Pisa, Italy ITALY
Corresponding Author Secondary Information:	
Corresponding Author's Institution:	Istituto Nazionale di Geofisica e Vulcanologia
Corresponding Author's Secondary Institution:	
First Author:	Alessio Di Roberto, Ph.D.
First Author Secondary Information:	
Order of Authors:	Alessio Di Roberto, Ph.D.
	Paola Del Carlo
	Sergio Rocchi
	Kurt Panter
Order of Authors Secondary Information:	
Abstract:	The ANtarctic geological DRILLing program (ANDRILL) successfully recovered 1138.54 m of core from drillhole, AND-2A, in the Ross Sea sediments (Antarctica). The core is composed of terrigenous claystones, siltstones, sandstones, conglomerates, breccias, and diamictites with abundant volcanic material. In this work we present sedimentological, morphoscopic, petrographic, and geochemical data on pyroclasts recovered from core AND-2A, which provide insights on eruption styles, volcanic sources, and environments of deposition. One pyroclastic fall deposit, 12 resedimented volcaniclastic deposits and 14 volcanogenic sedimentary deposits record a history of intense explosive volcanic activity in southern Victoria Land during the Early Miocene. Tephra were ejected during Subplinian and Plinian eruptions fed by trachytic to rhyolitic magmas and during Strombolian to Hawaiian eruptions fed by basaltic to mugearitic magmas in submarine/subglacial to subaerial environments. The long-lived Mt. Morning eruptive centre, located c. 80 km south of the drillsite, was recognized as the probable volcanic source for these products on the basis of volcanological, geochemical, and age constraints. The study of tephra in the AND-2A core provides important paleoenvironment information by revealing that the deposition of primary and moderately reworked tephra occurred in a proglacial setting under generally open-water marine conditions.

Cover Letter

Click here to download Cover Letter: Letter to Editor.docx

Early Miocene volcanic activity and paleoenvironment conditions recorded in tephra layers of the AND-2A core (southern McMurdo Sound, Antarctica).

Di Roberto A.[1], Del Carlo P.[1], Rocchi S.[2], Panter K. S.[3]

1 Istituto Nazionale di Geofisica e Vulcanologia, Sezione di Pisa, via della Faggiola 32, I 56126 Pisa, Italy;

2 Dipartimento di Scienze della Terra, Università di Pisa, Via S. Maria, 53, I-56126 Pisa, Italy;

3 Department of Geology, Bowling Green State University, Bowling Green, OH, 43403, USA;

Keywords:
Antarctica
volcaniclastic sediments
paleoenvironment
Mt. Morning
Victoria Land Basin

ABSTRACT

The ANtarctic geological DRILLing program (ANDRILL) successfully recovered 1138.54 m of core from drillhole, AND-2A, in the Ross Sea sediments (Antarctica). The core is composed of terrigenous claystones, siltstones, sandstones, conglomerates, breccias, and diamictites with abundant volcanic material. In this work we present sedimentological, morphoscopic, petrographic, and geochemical data on pyroclasts recovered from core AND-2A, which provide insights on eruption styles, volcanic sources, and environments of deposition. One pyroclastic fall deposit, 12 resedimented volcaniclastic deposits and 14 volcanogenic sedimentary deposits record a history of intense explosive volcanic activity in southern Victoria Land during the Early Miocene. Tephra were ejected during Subplinian and Plinian eruptions fed by trachytic to rhyolitic magmas and during Strombolian to Hawaiian eruptions fed by basaltic to mugearitic magmas in submarine/subglacial to subaerial environments. The long-lived Mt. Morning eruptive centre, located c. 80 km south of the drillsite, was recognized as the probable volcanic source for these products on the basis of volcanological, geochemical, and age constraints. The study of tephra in the AND-2A core provides important paleoenvironment information by revealing that the deposition of primary and moderately reworked tephra occurred in a proglacial setting under generally open-water marine conditions.

INTRODUCTION

Over the last few decades significant insight on paleoenvironmental conditions in southern Victoria Land have come from archives of sediments recovered in cores drilled both onshore and offshore (Barrett et al., 1998 and 2000; Hambrey and Barrett, 1993; Fielding and Thomson, 1999; Naish et al., 2007; Harwood et al., 2008). Recently, the ANtarctic geological DRILLing program (ANDRILL) successfully recovered sediments and geophysical data from 1138.54 meters of drill-core in the second AND-2A drill hole (southern McMurdo Sound; Florindo et al., 2008). The coring site is located in the Ross Sea, approximately 50 km NW of Hut Point Peninsula on Ross Island (77°45.488'S; 165°16.613'E; Fig. 1).

The AND-2A core sampled an almost continuous (98% recovery) sequence of sediments composed of lithologies including terrigenous claystones, siltstones, sandstones, conglomerates, breccias, and diamictites (Florindo et al., 2008; Panter et al., 2008). Fourteen lithostratigraphic units were identified on the basis of major changes in lithology recognized during core description (Fielding et al., 2011). Sediments were interpreted to represent a wide and complex spectrum of depositional environments and dynamic fluctuations in the Antarctic ice-sheet recorded in numerous cycles of glacial advance and retreat during the Early to Middle Miocene (Fielding et al., 2011; Passchier et al., 2011).

Results from $^{40}Ar/^{39}Ar$ radiometric dating of primary to moderately reworked tephra layers (Di Vincenzo et al., 2010) range in age from Early Miocene to Pleistocene (c. 20 to c. 0.08 Ma) and comprise an expanded and almost continuous section of Early to Middle Miocene sediments (c. 20 to c. 11.5 Ma), which has not been previously recorded by drilling in this region (Harwood et al., 2009).

In this paper we present sedimentological, morphoscopic, petrographic and geochemical data from tephra recovered in the AND-2A core. We also focus on some of the sedimentological aspects of the tephra in order to infer their depositional history. The results provide constraints on volcanic sources, eruptions styles and depositional paleoenvironments.

THE EREBUS VOLCANIC PROVINCE

The Erebus volcanic province in southern Victoria Land represents the largest area of exposed late Cenozoic volcanic rocks and the most complete record of alkaline volcanism in Antarctica (Kyle and Cole 1974; Kyle 1990a, b; Di Vincenzo et al., 2010). The Erebus volcanic province comprises several large volcanic centers built on the western flank of the intracontinental West Antarctic rift system in the McMurdo Sound region (Kyle, 1990b) that range in age from the Early Miocene (c. 19 Ma) to the present day (Fig. 1). Ross Island is the largest volcanic complex in the area and is formed by the active Mt. Erebus volcano, which is surrounded radially by the Mt. Terror, Mt. Bird and Hut Point Peninsula eruptive centers. Mt. Erebus is composed mostly of basanite and phonolite deposits (Kyle, 1977 and 1981; Kyle et al., 1992) that date back to 1.3 Ma (basanite dyke from Cape Barne; Esser et al., 2004). Mt. Bird and Mt. Terror are basanitic shield volcanoes that were active from 4.6 to 3.8 Ma and 1.7 to 1.3 Ma, respectively (Wright and Kyle, 1990a and b; Kyle and Muncy, 1989). Hut Point Peninsula is Pleistocene in age (c. 1.3 Ma) and consists of alkaline volcanism that is dominated by basanitic-hawaiitic cinder cones and a phonolite dome (Observation Hill) (Kyle, 1981).

To the south of Ross Island, the Erebus volcanic province is represented by White Island; a basanite to tephriphonolite shield volcano that was active as early as 7.65 Ma (Cooper et al., 2007). Recently, evidence for Late Miocene (c. 6.5 Ma) submarine to emergent volcanism was found in close proximity to White Island (Di Roberto et al., 2010). Farther south, Black Island, Minna Bluff, Mt. Morning and Mt. Discovery are all major eruptive centers belonging to Erebus volcanic province. The Minna Bluff peninsula and Black Island volcanic complexes are both composed of alkaline volcanic products belonging to the basanite-phonolite lineage and were active between c. 12 and 4 Ma (Fargo et al., 2008; Wilch et al., 2011) and between 11.2 and 1.7 Ma (Timms, 2006), respectively. Mt. Morning is the oldest volcanic complex in the Erebus volcanic province and has been divided into two phases of activity. Phase I (18.7 to 11.4 Ma) is dominated by mildly alkaline, mostly trachytic rocks, and Phase II (6.13 to 0.02 Ma) is composed of strongly alkaline rocks belonging to the basanite-phonolite lineage (Kyle and Muncy 1989; Wright and Kyle 1990c; Wright-Grassham 1987; Kyle, 1990a and b; Paulsen and Wilson, 2009; Martin, 2009; Martin et al., 2010).

North of Ross Island, Franklin and Beaufort islands represent remnants of alkaline volcanic edifices, with ages that range from Quaternary (90±66 ka; date from a seamount 10 km north of Franklin Island) to Late Miocene (6.80±0.05 Ma) (Rilling et al., 2009). In addition to the large volcanic edifices, the Erebus volcanic province includes several small volcanic centers and fields (Kyle and Cole, 1974; Kyle, 1990b). Numerous volcanic ash deposits are found within the hyper-arid Dry Valleys region of the Transantarctic Mountains, chiefly in the Royal Society Range and the Wright-Taylor Valleys. Most of these volcaniclastic deposits were reported to be Miocene to Pliocene in age with ^{40}Ar/^{39}Ar ages ranging from c. 15.15 to c. 4.33 Ma (Kyle and Cole, 1974; Kyle, 1990a; Marchant et al., 1996; Lewis et al., 2007). The Dailey Islands are c. 10 km south of the SMS drillsite and consist of heavily eroded remnants of basaltic cinder cones and lava deposits. Studies of volcanic rocks from two of the five islands reveal paleomagnetic normal polarities and radiometric ages of 0.78±0.04 Ma (Mankinen and Cox, 1988; Tauxe et al., 2004; Del Carlo et al., 2009). Finally, traces of the earliest activity within the Erebus volcanic province comes from volcaniclastic detritus and tephra recovered in the CIROS-1, MSSTS-1, Cape Roberts Project and AND-2A drillcores, which extends the volcanic history of the province back to ~26 Ma (Gamble et al., 1986; Barrett, 1987; McIntosh, 1998 and 2000; Acton et al., 2008; Di Vincenzo et al., 2010).

VOLCANIC ROCKS IN AND-2A CORE AND ANALYTICAL METHODS

Preliminary stratigraphic and petrologic data on volcanic products in the AND-2A core were reported in Fielding et al. (2008) and Panter et al. (2008), and provide the foundation for this study. The volcanic material in the AND-2A core includes dispersed clasts of lava, scoria fragments and pumices, variably reworked tephra layers and one primary tephra. More than 50% of the total clasts identified in 9 of the 14 lithostratigraphic units (LSU) are volcanic in origin and LSU 1 (0 to 37 meters below sea floor – m b.s.f) represents the most volcanic-rich unit within the core. The weakly reworked tephra beds, lava breccias and ripple cross-laminated vitroclastic sands in LSU 1 are interpreted to be deposited in a shallow marine environment by Strombolian- and Hawaiian-type volcanism from proximal volcanic sources (Del Carlo et al., 2009).

For this study, 27 volcaniclastic beds were identified and sampled from LSU 2 to LSU 14 (i.e. between 37.07 and 1138.54 m b.s.f; Table 1) and their sedimentological and volcanological characteristics are the basis for the interpretations presented in this paper. Because most of these samples are poorly lithified, they were impregnated with epoxy resin and prepared as standard polished thin sections for petrography and electron microprobe analysis. Observations of the sediments and sedimentary rocks were made using a stereomicroscope in order to detail sedimentologic structures and qualitatively identify sediment components and their relative abundance. This work led to the selection of samples for scanning electron microscopy and analysis by electron microprobe. Morphological and textural observations of components were performed by means of scanning electron microscopy (SEM) at Istituto Nazionale di Geofisica e Vulcanologia (Sezione di Pisa) using a Zeiss EVO MA 10 equipped with an Oxford ISIS microanalysis system. Major element glass composition and mineral analyses of glass-bearing volcanic fragments and alteration phases were performed at the HPHT Laboratory of Istituto Nazionale di Geofisica e Vulcanologia (Sezione di Roma) using a JEOL JXA 8200 microprobe equipped with 5 wavelength-dispersive spectrometers (WDS) and an energy-dispersive analyzer system (EDS). Instrumental conditions were: accelerating voltage 15 kV, beam current 5 nA, probe diameter 5 μm, acquisition time 10 s and 5 s for peak and background, respectively. Whenever possible, a minimum of 25 particles were analyzed in each sample. Relative standard errors for each element are reported in Supplemental Table 1.

RESULTS

The sampled deposits have been grouped into three types based on sedimentary features, the nature and abundance of components (Figs. 2 and 3), and on the major element compositions of glassy fragments (Fig. 5 and Table 2). They are: (i) pyroclastic fall deposits, (ii) resedimented volcaniclastic deposits, and (iii) volcanogenic sedimentary deposits (terminology after McPhie et al., 1993).

Pyroclastic fall deposit

A 6 cm-thick (640.13 and 640.19 m b.s.f) pyroclastic fall deposit was identified between within LSU9 (Panter et al., 2008; Di Vincenzo et al., 2010). The lapilli tuff is massive to faintly normally graded and contains a homogeneous distribution of pale green pumice fragments (<3 mm in diameter) set in matrix formed by angular glass shards that range in size from coarse to very fine ash. The lapilli tuff is under and overlain by volcanic-rich sandstones composed of light brown fresh volcanic glass shards, pale green to white altered glass shards, abundant lithic fragments (commonly of metasandstones and schists and less commonly of granite, dolerite and marble) and loose crystals (mainly quartz, feldspars and plagioclase).

The contact with the underlying sediment is sharp whereas the upper contact is gradational (Fig. 2A). Pale green pumices are moderately to highly vesicular (Houghton and Wilson, 1989) with a frothy morphology. Vesicles range in shape from spherical to elongated and are sometimes deformed (collapsed) or highly coalesced. Pumices are mostly aphyric with rare, K-feldspar phenocrysts (<2 mm), occasionally occurring with strongly green-colored clinopyroxene (<1 mm; optically determined aegirine/aegirine-augite). Angular glass shards are usually blocky, vesicle-free to poorly vesicular with vesicles ranging in shape from spherical to oblate (collapsed). A continuous spectrum of vesicularity exists between vesicle-free glass shards and highly vesicular pumice. Glass fragments forming the fine-grained part of the deposit (very fine ash) are variably vesicular (analogous to those described above) and range in shape from y-shaped to cuspate and blocky (Fig. 3A).

Most of the analyzed glass shards and pumice fragments are subtly to weakly altered with thin (<3 μm) transparent rims of leached glass at the surface of the grains and along fractures and vesicles (Fig. 3E). Well developed, pervasive perlitic fractures occur chiefly in dense, angular glass fragments (Fig. 3F). The deposit is cemented by calcite and clay minerals.

Resedimented volcaniclastic deposits

Twelve resedimented volcaniclastic deposits (defined in accordance with McPhie et al., 1993) were identified between 621.24 and 1093 m b.s.f (LSU9-13; Table 1). Two groups were distinguished within these deposits: (i) resedimented pumice- and scoria-rich sandstone to lapillistone (9 layers; Fig. 2B), and (ii) resedimented, strongly laminated, ash-rich mudstone to sandstone (3 layers; Fig. 2C). Resedimented pumice- and scoria-rich sandstone to lapillistone comprise grain-supported, <2 cm beds and lenses of pale green and clear, highly vesicular pumice mixed with scoria clasts made up of variably vesicular (from dense to pumiceous), light to dark yellow sideromelane and tachylite fragments (Fig. 3B). Clasts occur in a fine sand matrix, which is cross- to parallel-laminated at mm to cm scale. The matrix is composed of glass fragments with the same range of composition as the clasts, with crystals of K-feldspar, plagioclase, and quartz and lithic fragments (metasandstones and schists and less commonly of granite, dolerite and marble; Fig. 3B). Pumice and scoria fragments are in some cases abraded and subrounded. Deposits have sharp and planar contacts with the underlying sediments whereas upper contacts are gradational to diffuse; fragments with elongated shapes are commonly imbricated parallel to sand laminae or oriented along the lee side of ripple cross-laminations. Pumice are similar in vesiculatity, alteration degree (subtle to weak), and texture to those observed in the pyroclastic fallout deposit at 640.13-640.19 m b.s.f (Fig. 3A); they are mostly aphyric with minor K-feldspar phenocrysts (<2 mm), rarely accompanied by (<1 mm) strongly green-colored clinopyroxene (optically determined aegirine/aegirine-augite). A second population of pumice and glass shards, showing textures similar to those previously described but made of clear glass, was identified in five samples at 831.68, 953.28, 954.05, 1027.27 and 1093 m b.s.f, respectively, and rarely within sediments at shallower depths. Scoria clasts and light to dark yellow sideromelane and tachylite fragments are pumiceous to blocky to y-shaped (Figs. 2B and 3B). The scoria is weakly porphyritic with microphenocrysts of plagioclase, rare strongly green-colored clinopyroxene and minor olivine, apatite and magnetite set in a hypocrystalline groundmass. Glass is pristine to subtly altered with rims of palagonite to smectite a few microns-thick that line clasts or vesicles walls.

Resedimented, strongly laminated, ash-rich mudstone to sandstone consist of parallel laminated, rhythmic couplets of grain-supported fine sandstone to siltstone grading upward to mudstone. Couplets range in thickness from <1 mm to a few mm. Individual couplets have sharp lower and upper contacts whereas internal contacts between the volcaniclastic silt/sand and clay facies range from gradational to sharp (Figs. 2C and 3C). Volcaniclastic silt/fine sand laminae are composed of pale green, highly vesicular pumice fragments mixed with dense to pumiceous, light brown-colored sideromelane and tachylite fragments. Fragments are pristine and preserve thin vesicle glass walls and fragile structures. Minor amounts of loose crystals (<1 mm) of K-feldspar, plagioclase and quartz and lithics (commonly mafic lava fragments, granite dolerite and rarely schists) occur. Lapilli-sized pumice fragments and sedimentary intraclasts (siltstone) occur and are observed to load underlying clay laminae and be draped by laminae at the top.

Volcanogenic sedimentary deposits

Volcanogenic sedimentary deposits, namely shard-rich mudstones and sandstones (McPhie et al., 1993), were identified at several depths (LSU2-13; Table 1). This type of deposit includes intervals of < 2 mm, variably vesicular scoria, pale green and clear pumice set in sand to silt sized volcanic-rich matrix. Abundant lithic fragments (Figs. 2D and 3D) of most commonly volcanic rocks are recorded; they are mainly represented by variably vesicular lava with feldspar and < 2 mm, strongly green-colored clinopyroxene (optically determined aegirine/aegirine-augite) set in an intergranular to felted groundmass. Crystals of quartz, K-feldspar and biotite occur. Palagonitized glass shards and vesicular fragments were found in some samples. Rare, holocrystalline intrusive rocks are found that consist mainly of granitoids (quartz ± feldspar ± biotite ± hornblende) with hypidiomorphic to allotriomorphic and moderately deformed textures. Rare metamorphic lithic fragments were identified consisting of schist, gneiss, quartzite, and low-grade metasediments. Bioclasts are common and include foraminifera, shell fragments, spicules, diatoms and bryozoans (Fig. 3D). Irrespective of their origin (volcanic, metamorphic or biologic), fragments within vitric siltstone and sandstone are usually sub- to well-rounded. Lithologies of lithic fragments are similar to those of clasts described for the same interval by Panter et al. (2008) and Talarico et al. (2011) and a more detailed description of their characteristics and inference on their provenance the reader is referred to these papers.

Below 953.28 m b.s.f, the majority of glass fragments forming the volcanogenic sedimentary deposits are moderately to strongly altered. Most of the original textures have been modified or destroyed and volcanic glass is usually dissolved and replaced clay minerals, zeolites and carbonates. In some samples "pseudo-fiamme" clasts are common and are interpreted to have formed from burial compaction of lapilli-sized pumice clasts. Diffuse authigenic pyrite is found together with framboidal agglomerates of microscopic (<1 μm) isometric crystals of greigite (Fe_3S_4).

Chemistry of volcanic glass

A total of 600 glass fragments collected from throughout the length of the core have been analyzed (Table 2 and Supplemental Figure 1). The SiO_2 contents of glass range from c. 40 to c.73 wt.% and have been divided into two main compositional groups: 1) light brown-colored sideromelane and tachylite fragments with SiO_2 concentrations <52 wt.% and 2) pale green to colourless glass fragments with SiO_2 >63 wt.%. The majority of glass fragments within the second group are subtly to weakly altered and have low total oxides (<97 wt.%).

How the alteration effects the chemistry of volcanic glasses is examined semi-quantitatively by plotting their compositions in the "Alteration box plot" (Large et al., 2001) shown in Figure 4. The diagram combines the Alteration Index (AI) of Ishikawa et al. (1976) and the Chlorite-Carbonate-

Pyrite Index (CCPI) of Large et al. (2001) and was originally used with whole rock compositional data in volcanic-hosted massive sulfide deposits to discriminate hydrothermal alteration mineral assemblages from diagenetic assemblages. When used in combination with other compositional data and detailed petrographic and textural observations, the "Alteration box plot" gives an indication of alteration trends and processes.

Most of the low silica (52-63 wt.% SiO_2), light brown-colored sideromelane and tachylite fragments found within all sediment types within the depth interval between 621.24 and 831.68 m b.s.f. are pristine and plot within the least-altered rocks fields of the Alteration box plot (light blue diamonds in Fig. 4). A few compositions are marked by a decrease of the CCPI values (depletion of FeO + MgO versus Na_2O + K_2O; pink diamonds in Fig. 4) and likely indicate incipient hydrothermal alteration. Below 831.68 m b.s.f., the alteration of light brown-colored sideromelane and tachylite fragments increases further downcore with glass being progressively replaced by zeolites and clay minerals and glass shards destroyed by compaction and diagenetic processes.

Throughout the core, the majority of the high silica (> 63 wt.% SiO_2), pale green to colorless glass fragments is subtly to weakly altered. Above ~953 m b.s.f., the glasses show homogeneous AI values ranging between ~40 and ~55, whereas values of CCPI vary more broadly between ~35 and ~70 (red diamonds in Fig. 4). This indicates a rough increase of the CCPI values with respect to the relatively least-altered rocks (depletion of Na_2O + K_2O versus FeO + MgO), which is typical of hydrothermal alteration in the chlorite-dominated zone (Large et al., 2001). Below ~953 m b.s.f to the bottom of the core, glass compositions spread along the lower margin of the diagram having low CCPI values (<20) and a wide range of AI values (~15 to 80; purple diamonds in Fig.4).

Most of the pale green to colorless glass fragments that were initially considered unaltered (trachytic composition) plot across the lower margin of the Alteration Box Plot. Despite their high total oxides (>97 wt. %) they are interpreted to be subtly based on the slight depletion in FeO + MgO and variable depletion in Na_2O + K_2O + CaO (blue diamonds in Fig. 4).

The unaltered light brown-colored sideromelane and tachylite fragments range from basanite and basalt/tephrite to mugearite and overlap compositions of other basic volcanic rocks from the Erebus volcanic province (Fig. 5).

It is noteworthy that the pyroclastic fall deposit and resedimented volcaniclastic deposits have a narrow range of AI and CCPI values, whereas the volcanogenic sedimentary deposits show a broader range of values for these alteration indices. This could be attributed to the origin of each deposit type. For instance, the pyroclastic fall deposit and resedimented volcaniclastic deposits are considered to be composed of fragments emitted from the same source, transported together and deposited contemporaneously. Alternatively, the volcanogenic sedimentary deposits maybe a composite of products from multiple volcanic sources, with different transport and deposition dynamics, and thus would should show greater variability in their degree of alteration.

Factors influencing the alteration of volcanic glass include the nature of the aluminosilicate source material (e.g. glass vs. crystalline materials), the composition of original rock and of pore fluids, pH and the temperature, and porosity of sediments. None of these factors seem to explain why felsic glass shards dispersed within sediments are more altered than the coexisting basaltic ones. Felsic glass is considered to alter at a slower rate relative to mafic glass. The alteration seems to be related to the glass's viscosity, which in turn is a function of the composition and in particular H_2O and SiO_2 content (Gifkins et al., 2005 and reference therein). A possible explanation for why the basaltic glass is better preserved may be related to differences in the quenching (cooling) and hydration history of mafic versus felsic magmas (Marsaglia and Tazaki, 1992). Felsic magmas erupted in a water-rich environment (i.e. transitional or shallow water and subglacial) might have hydrated and altered more quickly than basaltic glass emitted in a water free (subaerial) environment.

DISCUSSION

Eruptive styles

Grain morphology, texture and vesicularity of pyroclasts are indicative of eruptive style and the environment in which the eruption occurred. Magmatic eruptions typically produce variably vesicular particles with cuspate to frothy morphologies, determined by viscosity, temperature, and volatile content (Cashman et al., 2000; Morrissey et al., 2000; Maria and Carey, 2002). Conversely phreatomagmatic eruptions produce dense to poorly vesicular, often fine-grained (<100μm) particles with a predominance of blocky morphologies (Cashman et al., 2000; Morrissey et al., 2000; Maria and Carey, 2002). Primary volcanic particle morphology can then be affected by post-eruptive reworking. Volcanic particles identified in the AND-2A core show a variety of morphologies and range from vesicle free to highly vesicular, suggesting they were formed from both magmatic and phreatomagmatic eruptions under a range of conditions, detailed below.

High-silica glass

The morphology and texture of highly vesicular pumice within the pyroclastic fall deposit and resedimented volcaniclastic deposits in AND-2A core are indicative of magmatic fragmentation processes. These products are emitted during energetic Subplinian and Plinian eruptions fed by silicic magmas. During these eruptions large amounts of highly vesicular pumice (60-93 volume %; Klug and Cashman, 1996; Cashman et al., 2000) and fine ashes are produced and carried in eruptive columns up to several tens of kilometers-high and dispersed by winds distances up to hundreds of kilometers from the source (Carey and Bursik, 2000).

In contrast, dense to poorly vesicular, fine-grained glass shards, with a predominance of blocky morphologies, with hydration cracks and perlitic fracturing textures, suggest phreatomagmatic fragmentation processes (Heiken and Wohletz, 1985 and 1991; Houghton and Wilson, 1989). Phreatomagmatic eruptions may occur in sub-marine and sub-lacustrine environments, or when magma comes into contact with groundwater or wet-sediment (Heiken and Fisher, 2000). In glacimarine environments like McMurdo Sound the most likely water sources for phreatomagmatic process are seawater and ice (Smellie, 2000).

Despite strong differences in morphology and vesicularity, the highly vesicular pumice and dense to poorly vesicular glass fragments have the same chemical composition (and degree of alteration) and coexist within the same layer, indicating that they may represent different fragmentation processes (magmatic versus phreatomagmatic) within a single eruption. In addition, as described above, a continuum between end member types which cover the whole spectrum of vesicularity occur within these layers. This is consistent with a volcanic eruption occurring in a transitional environment; i.e. evolving from shallow water or sub-glacial conditions (strong magma-water interaction) to a subaerial environment (no magma-water interaction). Alternatively, multiple vents located in subaerial and shallow subaqueous environments or a single vent experiencing rapid cycling between ‘dry’ Strombolian and ‘wet’ phreatomagmatic explosions during a single eruptive phase (Panter and Winter, 2008) may be invoked.

Low-silica glass

Sideromelane and tachylite fragments are frothy, blocky, y-shaped, or cuspate and vary from vesicle-free to highly vesicular. Most of the vesicular scoria observed are typical of weakly to mildly explosive Strombolian or Hawaiian style eruptions (Cashman et al., 2000). Strombolian eruptions consist of rhythmic, usually short-lived, mildly energetic explosions during which magmatic volatiles are released and significant amounts of ash- to bomb- sized materials are ejected to heights of a few hundred metres above a crater. Hawaiian style eruptions involve lava flows together with lava fountains typically tens to hundreds of metres height. Typically lava fountains are fed by basaltic magmas characterized by low viscosity, low volcanic gas content, and high temperature. Lava fountains eject pyroclasts ranging in size from millimeters to about one metre in diameter (Parfitt, 2004). Pyroclasts formed during Strombolian- and Hawaiian-style eruptions accumulate mainly as coarse, primary fallout deposits within a few kilometers of the vent. Only in the rare cases of strong magmatic fragmentation, for example during violent Strombolian or Plinian basaltic eruptions, can pyroclasts be dispersed hundreds of kilometers from the source.

As with high-silica glasses , the presence of basaltic particles that are dense to poorly vesicular and fine-grained with blocky morphologies in AND-2A pyroclastic fall and resedimented volcaniclastic deposits may indicate phreatomagmatic activity.

Volcanic source

Major element compositions of glass fragments combined with $^{40}Ar/^{39}Ar$ age data from the pyroclastic fall deposit and resedimented volcaniclastic deposits (see Table 1; age data from Di Vincenzo et al. 2010) provide information on the provenance of volcanic materials. The ages of studied AND-2A samples vary from c. 20 to 17.11 Ma (Early Miocene), according to $^{40}Ar/^{39}Ar$ age determinations of Di Vincenzo et al. (2010). Volcanic activity of comparable age occurred on the Malta Plateau in the Melbourne volcanic province (Armienti et al., 1991; Müller et al., 1991) and in the Erebus volcanic province at Mt. Morning (Kyle and Muncy, 1989; Wright and Kyle, 1990c; Wright-Grassham, 1987; Kyle, 1990a and b; Martin et al., 2010). In the Melbourne volcanic province, Middle Eocene magmatic activity is preserved in the form of multiple intrusions dated at 47.5 and 38.6 Ma (Tonarini et al., 1997; Rocchi et al., 2002). The oldest subaerial volcanic rocks crop out at Malta Plateau and Deception Plateau dated at c. 15 and 14 Ma (Armienti and Baroni, 1999). Dykes at Malta Plateau, possibly feeding lava flows, are dated between c. 18.2 and 14.1 Ma (Schmidt-Thomé et al., 1990). Although similar in composition and age, it is highly unlikely that Early to Middle Miocene volcanism in northern Victoria Land (Malta Plateau) is the source for AND-2A deposits simply because this activity occurred over 500 km north of the drillsite and the predominate wind and ice paleo-directions are inferred to have been in a northward direction in McMurdo Sound area (Sandroni and Talarico, 2006; Talarico and Sandroni, 2011). More likely, the volcanic source was to the south of the drillsite. The oldest Erebus volcanic province rocks crop out at Mt. Morning, where $^{40}Ar/^{39}Ar$ and K-Ar ages indicate that activity occurred in two phases: the first one between at least 18.7 Ma and 11.4 Ma and the second one between 6.13 and 0.02 Ma (Paulsen and Wilson, 2009; Martin, 2009; Martin et al., 2010). Evidence of volcanic activity pre-dating the onset of documented Mt. Morning volcanism was found in volcaniclastic detritus and tephra beds recovered in CIROS-1, MSSTS-1 and Cape Roberts (CRP) drillcores. The dates on these materials extend activity within the Erebus volcanic province back to c. 26 Ma (Gamble et al., 1986; Barrett, 1987; McIntosh, 1998 and 2000; Acton et al., 2008; Di Vincenzo et al., 2010). Volcanic activity older than c. 19 Ma can be ascribed to either a proto-Mt. Morning volcano buried under the present-day Mt. Morning edifice, or to an unknown volcanic centre, which has been eroded away or buried (Martin et al., 2010).

In Figures 5 and 6, major element compositions of glass fragments from the AND-2A core are compared with those of Early to Middle Miocene products sampled on land or in drillcores and attributed to the Erebus volcanic province (Armienti et al., 1998 and 2001; Pompilio et al., 2001; Kyle, 1981; Smellie, 1998). Only a limited number of glass compositions are available for McMurdo volcanics and the majority of data is from whole rocks. Nevertheless, the available data indicate that there is strong similarity between compositions of glass fragments in AND-2A core and some compositions of glass shards from volcaniclastic detritus and tephra beds recovered in CRP2/2A drillcores, which has already been attributed to the activity of the Erebus volcanic province (Armienti et al., 1998 and 2001; Smellie, 1998) and most likely sourced from Mt. Morning. Discrepancies in the FeO_{tot} content between CRP2/2A drillcores glasses and AND-2A core glass may be caused by minor alteration of the latter as indicated by the Alteration Box plot (Figs. 4 and 7).

According to Martin (2009) and Martin et al. (2010) only 7% of Mt. Morning Phase I products sampled are mafic whereas the remainder are felsic, specifically trachyte (79%) and rhyolite (14 %) in composition. Our work and ongoing studies on sediments from different depth intervals (Nyland, 2011) indicate that mafic glass is abundant throughout the AND-2A core. The fresh mafic glass have alkali basalt, basanite, tephrite and (less commonly) mugearite compositions (Fig. 5), overlapping those of McMurdo Volcanic Group igneous products (Fig. 5; Kyle, 1990a; Armienti et al., 1998; Rocchi et al., 2002; Nardini et al., 2009). At depths greater than 600 m b.s.f. the SiO_2 content of glass increases with increasing depth (Fig. 7). Unaltered basaltic compositions occur prevalently above ~800 m b.s.f; below this depth they are altered and replaced by clay minerals and zeolites. Glass compositions below ~840 m b.s.f show a shift towards higher SiO_2 contents, with the highest (c. 70 wt.%) occurring near the bottom of the core (Fig. 7).

Our results complement the findings of Martin (2009) and Martin et al. (2010), confirming the bimodal compositions of Mt. Morning products. However, we found that the abundance of basaltic glass in the AND-2A core to be much higher than the 7% estimated for Mt. Morning deposits. This suggests that during the period corresponding to Phase I activity at Mt. Morning, volcanism fed by mafic magmas was much more prevalent than previously documented in surface deposits. This discrepancy may be explained by the premise that present-day exposures on Mt. Morning may not be representative of all of the material erupted. It could well be that Miocene trachyte and rhyolite deposits on Mt. Morning, consisting of remnants of domes and welded pyroclastic flows, were more resistant to weathering and erosion than basaltic scoria or even basaltic lava flows.

On the basis of textural and geochemical information we can infer eruption dynamics and sources. Given that almost all studied samples consist of particles produced by a combination of subaerial and submarine/sub-glacial magmatic and phreatomagmatic explosive activity (i.e. highly vesicular pumice, basaltic vesicular scoria, and vesicle-free blocky fragments), we suggest three possible scenarios: (i) a single volcanic complex, set in a transitional environment (submarine/sub-glacial to subaerial) erupting products with bimodal composition (basaltic and trachytic-rhyolitic); (ii) two contemporaneously active volcanic complexes, both set in a transitional environment (submarine/sub-glacial to subaerial) and fed separately by basaltic and trachytic-rhyolitic magmas; (iii) multiple contemporaneously active volcanic vents located in a range of environments (submarine/sub-glacial to subaerial) and fed by basaltic and trachytic-rhyolitic magmas.

Paleoenvironment implications

Volcaniclastic deposits are an important component of sedimentary successions and are valuable paleoenvironmental indicators. In marine and glacimarine environments, pyroclastic fall deposits may result from subaerial volcanic activity and particle settling through a water column or by direct transformation of gas-supported pyroclastic flow into a water-saturated gravity flow (Schneider et al., 2001). Primary volcaniclastic deposits can also originate from submarine volcanic activity ranging in styles from explosive to effusive (White, 2000). Resedimented volcaniclastic deposits may result from reworking and resedimentation of pyroclasts previously erupted on land (including supra-glacial, en-glacial and sub-glacial debris) or on sea ice.

Volcanic detritus is persistent and abundant throughout the AND-2A core, representing the dominant clast type in 9 of the 14 lithostratigraphic units (Panter et al., 2008). Apart from LSU1 (Del Carlo et al., 2009), volcanic material within the uppermost half of the core (to 608.35 m b.s.f) consists mostly of lava, scoria and pumice clasts dispersed in coarse-grained deposits (e.g., conglomerate, diamictite) and reworked glass in sandstone, siltstone and mudstone. The absence of pyroclastic fall deposits and resedimented volcaniclastic deposits in the upper part of the core may be explained by a combination of: (i) source, type and intensity of volcanic activity, (ii) ice extent and environmental conditions within the McMurdo Sound at the time of deposition or (iii) erosional processes.

During the period between c. 17.1 and 11.5 Ma when sediments were being deposited in the upper 600 m of the core (Di Vincenzo et al., 2010), volcanic activity in southern Victoria Land may have been less energetic (limited areal dispersion of ejecta), thus resulting in the lack of any discrete tephra beds at the coring site. Eruptions may have been prevalently submarine or sub-glacial and characterized by a limited dispersal of pyroclasts, as typically occurs for these types of eruptions. However, this hypothesis seems to be in contrast with the recent findings of Martin et al. (2010), that showed the presence of an intense and predominantly subaerial volcanic activity producing lava flows and pyroclastic deposits at Gandalf Ridge (18.7±0.3 and 15.5±0.5 Ma), Pinnacle Valley (15.4±0.1 and 13.0±0.3 Ma) and Mason Spur (12.9±0.1 and 11.4±0.2 Ma) that are located ~80 km from the coring site. In addition this also seems to be in conflict with findings of Marchant et al.

(1996) and Lewis et al. (2007), which have documented mafic to felsic ash layers in the Dry Valleys that are dated between 11 and 15 Ma. An alternative explanation is that the presence of thick ice-sheets in the Ross Sea embayment, with grounding lines located north of the present day positions, could have hampered the direct delivery of wind-driven volcanic materials to the coring site (ii. glacial paleoenvironmental conditions). Sedimentological and isotopic studies of sedimentary records demonstrate that changes in paleoenvironmental conditions occurred between c. 17.1 and 11.5 Ma (Zachos et al., 2008; Passchier et al., 2011) and these were accompanied by strong ice sheet fluctuations with multiple cycles of advance and retreat, which could possibly have allowed the deposition of pyroclastic fall deposit. Pyroclastic fall deposit and resedimented volcaniclastic deposits may have been eroded during the deposition of massive, coarse-grained deposits (diamictite and conglomerates) in sub-glacial to pro-glacial environments.

Volcanic material within the bottom half of the core, >600 m b.s.f., consists of dispersed lava clasts, scoria fragments, pumice, one pyroclastic fall deposit and at least ten resedimented volcaniclastic deposits. Products forming the 6 cm-thick lapilli tuff at 640 m b.s.f., which is dated at 17.4 Ma (Di Vincenzo et al., 2010), were most likely transported in an eruptive ash cloud and deposited directly through the water column. This would only be possible if open marine or partly-open marine conditions prevailed at the time (Fig. 8). Rounding and abrasion of dispersed pumice and scoria indicate that they spent some time as floating rafts prior to sinking, or transported on the seafloor prior to deposition, or have undergone weathering and re-sedimentation prior to their final deposition (Fig. 8). Limited mixing with fragments from non-volcanic material and imbrication of clast parallel to sand laminae or oriented along the lee side of ripple cross-laminations, suggest deposition by low energy volcaniclastic bottom or turbidity currents. Resedimented pumice- and scoria-rich sandstone to lapillistone can be considered indicators of open water conditions with limited sea ice, similar to the pyroclastic fall deposit at c. 640 m b.s.f. Resedimented, strongly laminated, ash-rich mudstone to sandstone found at ~636 and ~1027 m b.s.f are comparable with deposits generated by suspension settling from ice-proximal, turbid, melt water plumes (Ó Cofaigh et al., 2001 and references therein), observed in fjord environments, and more rarely, in high-latitude open marine settings. The absence of grain rounding, the preservation of fragile structures, and the low degree of post-eruptive sediment mixing with non-volcanic detritus all indicate that no significant reworking has occurred. We suggest that these pyroclasts were transported in eruptive columns, dispersed by wind onto the ice (glaciers) and finally released to the water column during repeated melting events. We therefore conclude that deposition of resedimented, strongly laminated, ash-rich mudstone to sandstone occurred in a pro-glacial setting with general open marine conditions. Similar depositional and dispersal processes have long been suggested for modern volcanogenic sediments in McMurdo Sound (Bentley, 1979; Barrett et al., 1983; Macpherson, 1987; Atkins and Dunbar, 2009).

CONCLUSIONS

The sedimentological, morphoscopic, petrological and geochemical study of pyroclasts recovered in AND-2A core has provided information about their volcanic sources and eruptions styles and new insights into their environment of deposition. One pyroclastic fall deposit and several resedimented, volcaniclastic deposits recovered in AND-2A core record an intense and recurrent history of volcanic activity in southern Victoria Land region during the Early Miocene. Two main explosive eruptive styles and magma compositions were recognised. Subplinian and Plinian eruptions involved trachytic to rhyolitic magmas, while Strombolian to Hawaiian eruptions were fed by basaltic to mugearitic magmas. In both cases the occurrence of vesicle-free, blocky fragments indicates that hydromagmatic fragmentation processes were caused by the interaction of magmas with seawater and/or glacial meltwater within a glacimarine environment. On the basis of the available geochemical and chronological data and using volcanological constraints, we infer that the proto-Mt. Morning and Mt. Morning volcanoes located south of the drillsite are the most likely volcanic sources. Finally, the sedimentological features of the volcanic units are interpreted to indicate that they were deposited in a pro-glacial setting with overall open-water marine conditions.

ACKNOWLEDGMENTS

The ANDRILL Program is a multinational collaboration between the Antarctic Programs of Germany, Italy, New Zealand and the United States. Antarctica New Zealand is the project operator, and has developed the drilling system in collaboration with Alex Pyne at Victoria University of Wellington and Webster Drilling and Enterprises Ltd. Scientific studies are jointly supported by the US National Science Foundation, NZ Foundation for Research Science and Technology, Royal Society of New Zealand Marsden Fund, the Italian Antarctic Research Program, the German Research Foundation (DFG) and the Alfred Wegener Institute for Polar and Marine Research (Helmholtz Association of German Research Centers). Antarctica New Zealand supported the drilling team at Scott Base; Raytheon Polar Services supported the science team at McMurdo Station and the Crary Science and Engineering Laboratory. The ANDRILL Science Management Office at the University of Nebraska-Lincoln provided science planning and operational support. ADR benefited of a post-doc grant from PNRA. Authors are grateful to Co-Chiefs F. Florindo and D. Harwood and the Science Team (http://www.andrill.org) of the SMS ANDRILL project. A. Cavallo is kindly acknowledged for the assistance during microprobe analyses. S. Petrushak is kindly acknowledged for collecting samples of AND-2A core at Antarctic Marine Research Facility at Florida State University. A.P. Martin and anonymous reviewers are also acknowledged for their accurate and critical revision of the manuscript.

REFERENCES CITED

Acton, G.; Crampton, J.; Di Vincenzo, G.; Fielding, Christopher R.; Florindo, F.; Hannah, M.; Harwood, D. M.; Ishman, S.; Johnson, K.; Jovane, L.; Levy, Richard; Lum, B.; Marcano, M. C.; Mukasa, S.; Ohneiser, C.; Olney, M. P.; Riesselman, C.; Sagnotti, L.; Stefano, C.; Strada, E.; Taviani, M.; Tuzzi, E.; Verosub, K. L.; Wilson, G. S.; Zattin, M.; and ANDRILL-SMS Science Team, 2008, Preliminary integrated chronostratigraphy of the AND-2A core, ANDRILL Southern McMurdo Sound Project. *in* Harwood, D.M., Florindo, F., Talarico, F., Levy, R.H., eds., Studies from the ANDRILL, Southern McMurdo Sound Project, Antarctica: Terra Antartica, v. 15, 211-220.

Armienti, P., and Baroni, C., 1999, Cenozoic climatic change in Antarctica recorded by volcanic activity and landscape evolution: Geology, v. 27, p. 617-620.

Armienti, P., Civetta, I., Innocenti, F., Manetti, P., Tripodo, A., Villari, L., and Vita, G., 1991, New petrographical and geochemical data on Mt. Melbourne volcanic field, Northern Victoria Land, Antarctica: Memorie della Società Geologica Italiana, v. 46, p. 397-424.

Armienti, P., Messiga, B. and Vannucci, R., 1998, Sand provenance from major and trace element analyses of bulk rock and sand grains: Terra Antartica, v. 5, p. 589-599.

Armienti, P., Tamponi, M., and Pompilio, M., 2001, Petrology and provenance of volcanic clasts, sand grains and tephras: Terra Antartica, v. 8, p. 2-23.

Armstrong, R.L., 1978, K-Ar dating: Late Cenozoic McMurdo Volcanic Group and Dry Valley glacial history, Victoria Land, Antarctica: New Zealand Journal of Geology and Geophysics, v. 21, p. 685–698.

Armstrong, R.L., Hamilton, W., and Denton, G.H., 1968, Glaciation in Taylor Valley, Antarctica, older than 2-7 million years, Science, v. 159, p. 187-188.

Atkins, C.B., and Dunbar, G.B., 2009, Aeolian sediment flux from sea ice into Southern McMurdo Sound (SMS), Antarctica: Global and Planetary Change, v. 69, p. 133-141.

Barrett, P.J., 1987, Oligocene sequence cored at CIROS-1, western McMurdo Sound: New Zealand Antarctic Record, v. 7, p. 1–17.

Barrett, P.J., Fielding, C.R., and Sherwood W., 1998, Initial report on CRP-1, Cape Roberts Project, Antarctica: Terra Antarctica, v. 5(1), 187 p., hdl:10013/epic.28286.d001

Barrett, P.J., Pyne, A.R., and Macpherson, A.J., 1983, Observations of the sea floor of McMurdo Sound and Granite Harbour: New Zealand Antarctic Record, v. 5, p. 16–22.

Barrett, P.J., Sarti, M, and Sherwood, W., 2000, Studies from the Cape Roberts Project, Ross Sea, Antarctica, Initial Reports on CRP-3: Terra Antarctica, v. 7, 209 p.

Bentley, P.N., 1979, Characteristics and distribution of windblown sediment, Western McMurdo Sound, Antarctica. [BSc. Hons Thesis]: Wellington, Victoria University of Wellington, New Zealand.

Carey, S., and Bursik, M., 2000, Volcanic plumes, *in in* Sigurdsson, H., Houghton, B.F., McNutt, S.R., Rymer, H., and Stix, J., eds.., Encyclopedia of Volcanoes: San Diego, U.S., Academic Press, p. 527-544.

Cashman, K.V., Sturtevant, B., Papale, P., and Navon, O., 2000, Magmatic fragmentation, *in* Sigurdsson, H., Houghton, B.F., McNutt, S.R., Rymer, H., and Stix, J., eds., Encyclopedia of Volcanoes: San Diego, U.S., Academic Press, p. 421-430.

Cooper, A.F., Adam, L.J., Coulter, R.F., Eby, G.N., and McIntosh, W.C., 2007, Geology, geochronology and geochemistry of a basanitic volcano, White Island, Ross Sea, Antarctica: Journal of Volcanology and Geothermal Research, v. 165, p. 189-216, doi: 10.1016/j.jvolgeores.2007.06.003.

Del Carlo, P., Panter, K.S., Bassett, K., Bracciali, L., Di Vincenzo, G., and Rocchi, S., 2009, The upper lithostratigraphic unit of ANDRILL AND-2A core (Southern McMurdo Sound, Antarctica): Local volcanic sources, paleoenvironmental implications and subsidence in the western Victoria Land Basin: Global and Planetary Change, v. 69, p. 142-161, doi: 10.1016/j.gloplacha.2009.09.002.

Di Roberto, A., Pompilio, M., and Wilch, T.I., 2010, Late Miocene submarine volcanism in ANDRILL AND-1B drill core, Ross Embayment, Antarctica: Geosphere, v. 6, p. 524-536, doi: 10.1130/GES00537.1.

Di Vincenzo, G., Bracciali, L., Del Carlo, P., Panter, K., and Rocchi, S., 2010, $^{40}Ar/^{39}Ar$ laser dating of volcanogenic products from the AND-2A core (ANDRILL Southern McMurdo Sound Project, Antarctica): Bulletin of Volcanology, v. 72, p. 487–505, doi: 10.1007/s00445-009-0337-z.

Esser, R.P., Kyle, P.R., and McIntosh, W.C., 2004, $^{40}Ar/^{39}Ar$ dating of the eruptive history of Mt. Erebus, Antarctica: Volcano evolution: Bulletin of Volcanology, v. 66, p. 671–686, doi: 10.1007/s00445-004-0354-x.

Fargo, A.J., McIntosh, W.C., Dunbar, N.W., and Wilch, T.I., 2008, $^{40}Ar/^{39}Ar$ geochronology of Minna Bluff, Antarctica: Timing of mid-Miocene glacial erosional events within the Ross Embayment [abs.] Eos (Transactions, American Geophysical Union), v. 89(53), Fall Meeting Supplement.

Fielding C.R., Browne, G.H., Field, B., Florindo, F., Harwood, D.M., Krissek, L.A.,. Levy, R.H., Panter, K.S., Passchier, S., Pekar, S.F., 2011, Sequence stratigraphy of the ANDRILL AND-2A drillcore, Antarctica: A long-term, ice-proximal record of Early to Mid-Miocene climate, sea-level and glacial dynamism: Palaeogeography, Palaeoclimatology, Palaeoecology, v. 305, p. 336-351, doi: 10.1016/j.palaeo.2011.03.026

Fielding, C.R. and Thomson, M.R.A., 1999, Studies from the Cape Roberts Project, Ross Sea Antarctica, Initial Report on CRP-2/2A: Terra Antartica, Bremerhaven, PANGAEA, 6 (1), 173 pp.

Florindo, F., Harwood, D., and Levy, R. 2008. ANDRILL's Success During the 4th International Polar Year: Scientific Drilling, v. 6, p. 29-31. doi:10.2204/iodp.sd.6.03.2008.

Gamble, J.A., Barrett, P.J., and Adams, C.J., 1986, Basaltic clasts from Unit 8: Bulletin of New Zealand, v. 237, p. 145-152.

Gifkins, C.C., Herrmann, W., and Large, R.R., 2005 editors, Altered volcanic rocks: a guide to description. Centre for Ore Deposit Research, University of Tasmania. 275 pp.

Hambrey, M.J., and Barrett P.J., 1993, Cenozoic sedimentary and climatic record, Ross Sea region, Antarctica, *in* Kennett, J.P., and Warnke, D.A., eds, The Antarctic Paleoenvironment: A Perspective on Global Change: Part Two, Antarctic Research Series, v. 60, Washington, D.C, American Geophysical Union, pp. 91–124, doi:10.1029/AR060p0091.

Harwood, D.M., Florindo, F., Talarico, F., Levy, R.H., editors, 2008, Studies from the ANDRILL, Southern McMurdo Sound Project, Antarctica: Terra Antartica, v. 15, 253 pp.

Harwood, D.M., Florindo, F., Talarico, F., Levy, R.H., Kuhn, G., Naish, T., Niessen, F., Powell, R., Pyne, A., and Wilson, G., 2009, Antarctic drilling recovers stratigraphic records from the continental margin: Eos (Transactions, American Geophysical Union), v. 90, no. 11, p. 90-91, doi: 10.1029/2009EO110002.

Heiken, G.H., and Fisher, R.V., 2000, Water and magma can mix - A history of the concepts of hydrovolcanism (1819 - 1980), *in* Negendank, J.F.W. and Brüchmann, C., eds., International Maar Conference: Germany: Terra Nostra, v. 6, p. 165-189.

Heiken, G.H., and Wohletz, K.H., 1985, Volcanic ash: Berkeley, U.S., University of California Press, , CA. 245 pp.

Heiken G.H., and Wohletz, K, 1991, Fragmentation processes in explosive volcanic eruptions. *in* Fisher, R.V., and Smith, G., eds Sedimentation in Volcanic Settings: Society of Sedimentary Geology Special Publication, v. 45, p. 19-26.

Houghton, B.F., and Wilson, C.J.N., 1989, A vesicularity index for pyroclastic deposits: Bulletin of Volcanology, v. 51, p. 451-462.

Ishikawa, Y., Sawaguchi, T., Iwaya, S. and Horiuchi, M., 1976, Delineation of prospecting targets for Kuroko deposits based on modes of volcanism of underlying dacite and alteration haloes: Mining Geology, v. 26, p. 105-117.

Klug, C., and Cashman K.V., 1996, Permeability development in vesiculating magmas: implications for fragmentation: Bulletin of Volcanology, v. 58, p. 87-100.

Kyle, P.R., 1977, Mineralogy and glass chemistry of recent volcanic ejecta from Mt. Erebus, Ross Island, Antarctica: New Zealand Journal of Geology and Geophysics, v. 20, p. 1123-1146.

Kyle, P.R., 1981, Mineralogy and geochemistry of a basanite to phonolite sequence at Hut Point Peninsula, Antarctica, based on core from Dry Valley Drilling Project Drillholes 1, 2 and 3: Journal of Petrology, v. 22, p. 451-500.

Kyle, P.R, 1982, Volcanic geology of the Pleiades, Northern Victoria Land, Antarctica, *in* Craddock C., ed., Antarctic Geoscience: Madison,University of Wisconsin Press, p. 747-754.

Kyle, P.R., 1990a, McMurdo Volcanic Group – Introduction. *in* LeMasurier, W.E., and Thomson, J.W., eds., Volcanoes of the Antarctic plate and southern oceans: American Geophysical Union, Antarctic Research Series, v. 48, p. 19-25

Kyle, P.R., 1990b, Erebus Volcanic Province - Summary. *in* LeMasurier, W.E., and Thomson, J.W., eds., Volcanoes of the Antarctic plate and southern oceans: American Geophysical Union, Antarctic Research Series, v. 48, p. 81-35

Kyle, P.R., and Cole, J.W., 1974, Structural control of volcanism in the McMurdo Volcanic Group, Antarctica: Bulletin of Volcanology, v. 38, p. 16-25.

Kyle, P.R., Moore, J.A., and Thirwall, M.F., 1992, Petrologic evolution of anorthoclase phonolite lavas at Mt. Erebus, Ross Island, Antarctica: Journal of Petrology, v. 33, p. 849-875.

Kyle, P.R., and Muncy, H.L., 1989, Geology and geochronology of McMurdo Volcanic Group rocks in the vicinity of Lake Morning, McMurdo Sound, Antarctica: Antarctic Science, v. 1, p. 345–350, doi: 10.1017/S0954102089000520.

Large, R.R., Gemmell, J.B., Paulick, H., and Huston, D.L., 2001, The alteration box plot: a simple approach to understanding the relationship between alteration mineralogy and lithogeochemistry associated with volcanic-hosted massive sulfide deposits: Economic Geology, v. 96, p. 957–971.

LeMaitre, R.W., 1989, ed., A Classification of Igneous Rocks and Glossary of Terms: Blackwell Science, 193 pp.

LeMasurier, W.E. and Thomson, J.W., eds., 1990, Volcanoes of the Antarctic Plate and Southern Oceans: Washington, D.C., American Geophysical Union, Antarctic Research Series, v. 48, 512 pp.

Lewis, A.R., Marchant, D.R., Ashworth, A.C., Hemming, S.R. and Machlus, M.L., 2007, Major middle Miocene global climate change: evidence from East Antarctica and the Transantarctic Moutains: Geological Society of America Bulletin. doi:10.1130B26134.1.

Macpherson, A.J., 1987, The MacKay Glacier/Granite Harbour system (Ross Dependency, Antarctica). A study in nearshore glacial marine sedimentation. [Thesis]: Wellington, Victoria University of Wellington, New Zealand, 85 pp.

Mankinen, E.A., and Cox, A., 1988, Paleomagnetic investigation of some volcanic rocks from the McMurdo volcanic province, Antarctica: Journal of Geophysical Research, v. 93, p. 599-612.

Marchant, D.R., Denton, G.H., Swisher III, C.C. and Potter, N. Jr., 1996, Late Cenozoic Antarctic paleoclimate reconstructed from volcanic ashes in the Dry Valleys region of southern Victoria Land: Geological Society of American Bulletin, v. 108, p. 181–194.

Maria, A., and S. Carey, 2002, Using fractal analysis to quantitatively characterize the shapes of volcanic particles, Journal of Geophysical Research, v. 107, p. 2283-2300, doi:10.1029/2001JB000822.

Marsaglia, K.M., and Tazaki, K., 1992, Diagenetic trends in Leg 126 sandstones *in* Proceedings of the Ocean Drilling Program, Scientific Results: College Station, Texas A & M University, p. 125-138.

Martin, A.P., 2009, Mt. Morning, Antarctica: Geochemistry, geochronology, petrology, volcanology, and oxygen fugacity of the rifted Antarctic lithosphere [PhD thesis]: Dunedin, University of Otago,.

Martin, A., Cooper, A., and Dunlap, W., 2010, Geochronology of Mt. Morning, Antarctica: two-phase evolution of a long-lived trachyte-basanite-phonolite eruptive center: Bulletin of Volcanology, v. 72, p. 357-371, doi: 10.1007/s00445-009-0319-1.

Mayewski, P.A., 1975, Glacial geology and late Cenozoic history of the Transantarctic Mountains, Antarctica: Institute of Polar Studies, Report N°. 56, Ohio State University.

McIntosh, W.C., 1998, $^{40}Ar/^{39}Ar$ geochronology of volcanic clasts and pumice in CRP-1 core, Cape Roberts, Antarctica: Terra Antartica, v. 5, p. 683-690.

McIntosh, W.C., 2000, ^{40}Ar–^{39}Ar geochronology of tephra and volcanic clasts in CRP-2A,Victoria Land Basin, Antarctica: Terra Antartica, v. 7, p. 621-630.

McKelvey, B.C., Webb, P.N., Harwood, D.M. and Mabin, M.C.G., 1991, The Dominion Range Sirius Group: a record of the late Pliocene–early Pleistocene Beardmore Glacier, *in* Thomson, M.R.A., Crame, J.A., and Thomson, J.W., eds., Geological Evolution of Antarctica: Cambridge University Press, p. 675-682.

McPhie, J., Doyle, M., Allen, R.L., editors 1993, Volcanic Textures: A guide to the interpretation of textures in volcanic rocks: University of Tasmania, Centre for Ore Deposit and Exploration Studies, 198 pp.

Mercer, J.H., 1968, Glacial geology of the Reedy glacier area, Antarctica: Geological Society of American Bulletin, v. 79, p. 471-486.

Morrissey, M., Zimanowski, B., Wohletz, K., Buettner, R., 2000, Phreatomagmatic fragmentation, *in* Sigurdsson, H., Houghton, B.F., McNutt, S.R., Rymer, H., and Stix, J., eds., Encyclopedia of Volcanoes: San Diego, Academic Press, p. 231-245.

Müller, P., Schmidt-Thomé, M., Kreuzer, H., Tessensohn, F. and Vetter U., 1991, Cenozoic peralkaline magmatism at the western margin of the Ross Sea, Antarctica: Memorie della Società Geologica Italiana, v. 46, p. 315-336.

Muncy, H.L., 1979, Geologic history and petrogenesis of alkaline volcanic rocks, Mt. Morning, Antarctica [Thesis]: Ohio State University, 224 pp.

Naish T., Powell R. and Levy R. H., editors, 2007, Studies from the ANDRILL, McMurdo Ice Shelf Project, Antarctica – Initial Science Report on AND-1B: Terra Antartica, 14, 328 pp.

Nardini, I, Armienti, P., Rocchi, S., Dallai, L., and Harrison, D., 2009, Sr-Nd-Pb-He-O isotope and geochemical constraints on the genesis of cenozoic magmas from the West Antarctic Rift: Journal of Petrology, v. 50, p. 1359-1375.

Nyland, R., 2011, Evidence for early-phase explosive basaltic volcanism at Mt. Morning from glass-rich sediments in the ANDRILL AND-2A core and possible response to glacial cyclicity [MSc Thesis]: Bowling Green State University, USA.

Ó Cofaigh, C., and Dowdeswell, J.A., 2001, Laminated sediments in glacimarine environments: Diagnostic criteria for their interpretation: Quaternary Science Reviews, v. 20, p. 1411-436.

Panter, K.S., Talarico, F., Bassett, K., Del Carlo, P., Field, B., Frank, T., Hoffman, S., Kuhn, G., Reichelt, L., Sandroni, S., Tavini, M., Bracciali, L., Cornamusini, G., von Eynatten, H., and Rocchi, R., 2008, Petrologic and geochemical composition of the AND-2A core, ANDRILL Southern McMurdo Sound Project, Antarctica, *in* Harwood, D.M., Florindo, F., Talarico, F., and Levy, R.H., eds., Studies from the ANDRILL, Southern McMurdo Sound Project, Antarctica: Terra Antarctica, v. 15, p. 147-192.

Panter, K.S. and Winter, B., 2008, Geology of the side crater of the Erebus volcano, Antarctica: Journal of Volcanology and Geothermal Research, v. 177, p. 578-588.

Parfitt, E.A., 2004, A discussion of the mechanisms of explosive basaltic eruptions: Journal of Volcanology and Geothermal Research, v. 134, p. 77–107.

Passchier, S., Browne, G., Field, B., Fielding, C.R., Krissek, L.A., Panter, K., Pekar, S.F., and ANDRILL-SMS Science Team, 2011, Early and middle Miocene Antarctic glacial history from the sedimentary facies distribution in the AND-2A drill hole, Ross Sea, Antarctica: Geological Society of America Bulletin, doi:10.1130/B30334.1.

Paulsen, T.S. and Wilson T.J., 2009, Structure and age of volcanic fissures on Mount Morning: A new constraint on Neogene to contemporary stress in the West Antarctic Rift, southern Victoria

Land, Antarctica, Geological Society of America Bulletin, v. 121. p. 1071-1088; doi: 10.1130/B26333.1.

Pompilio, M., Armienti, P., and Tamponi, M., 2001, Petrography, Mineral Composition and Geochemistry of Volcanic and Subvolcanic Rocks of CRP-3, Victoria Land Basin, Antarctica: Terra Antartica, v. 8, p. 469-480.

Rilling, S., Mukasa, S., Wilson, T., Lawver, L., and Hall C., 2009, New determinations of 40Ar/39Ar isotopic ages and flow volumes for Cenozoic volcanism in the Terror Rift, Ross Sea, Antarctica: Journal of Geophysical Research, v. 114, doi:10.1029/2009JB006303.

Rocchi, S., Armienti, P., D'Orazio, M., Tonarini, S., Wijbrans, J.R. and Di Vincenzo, G., 2002, Cenozoic magmatism in the western Ross Embayment: Role of mantle plume versus plate dynamics in the development of the West Antarctic Rift System: Journal of Geophysical Research, v. 107 , 10.1029/2001JB000515.

Sandroni, S., and Talarico, F.M., 2006, Analysis of clast lithologies from CIROS-2 core, New Harbour, Antarctica-Implications for ice flow directions during Plio-Pleistocene time: Palaeogeography, Palaeoclimatology, Palaeoecology, v. 231, p. 215-232.

Schmidt-Thomé, M., Mueller, P., and Tessensohn, F., 1990, McMurdo Volcanic Group-western Ross Embayment: Malta Plateau: Antarctic Research Service, v. 48, p. 53-59.

Schneider, J.L., Le Ruyet, A., Chanier, F., Buret, C., Ferriere, J., Proust, J.N., and Rosseel, J.B, P., 2001, Primary or secondary distal volcaniclastic turbidites: how to make the distinction? An example from the Miocene of New Zealand (Mahia Peninsula, North Island), Sedimentary Geology, v. 145, p. 1-22, doi: 10.1016/S0037-0738(01)00108-7.

Smellie, J.L., 1998, Sand grain detrital modes in CRP-1: provenance variations and influence of Miocene eruptions on the marine record in the McMurdo Sound region: Terra Antartica, v. 5, p. 579-587.

Smellie, J.L., 2000, Subglacial eruptions. *in* Sigurdsson, H., Houghton, B., Rymer, H., Stix, J., and McNutt, S., eds., Encyclopedia of Volcanoes, San Diego, U.S., Academic Press, p. 403-418.

Talarico, F., Pace, D., and Sandroni, S., 2011, Amphibole-bearing metamorphic clasts in ANDRILL AND-2A core: A provenance tool to unravel the Miocene glacial history in the Ross Embayment (western Ross Sea, Antarctica): Geosphere, v. 7, p. 922-937, doi: 10.1130/GES00653.1.

Talarico, F., and Sandroni, S., 2011, Early Miocene basement clasts in ANDRILL AND-2A core and their implications for paleoenvironmental changes in the McMurdo Sound region (western Ross Sea, Antarctica): Global and Planetary Change, v. 78, p. 23-35, doi:10.1016/j.gloplacha.2011.05.002.

Tauxe, L., Gans, P., and Mankinen, E.A., 2004, Paleomagnetism and $^{40}Ar–^{39}Ar$ ages from volcanics extruded during the Matuyama and Brunhes Chrons near McMurdo Sound, Antarctica: Geochemistry, Geophysics, Geosystems (G3), v. 5, doi:10.1029/2003GC000656.

Timms, C., 2006, Reconstruction of a grounded ice sheet in McMurdo Sound - evidence from southern Black Island, Antarctica [MSc Thesis] Dunedin, University of Otago, 146 pp.

Tonarini, S., Rocchi, S., Armienti, P., and Innocenti, F., 1997, Constraints on timing of Ross Sea rifting inferred from Cenozoic intrusions from northern Victoria Land, Antarctica, *in* Ricci, C.A., ed., The Antarctic Region: Geological Evolution and Processes, p. 511-521.

White, J.D.L., 2000, Subaqueous eruption-fed density currents and their deposits: Precambrian Research, v., 101, p. 87-109

Wilch, T.I., Lux, D.R., Denton, G.H., and McIntosh, W.C., 1993, Minimal Pliocene–Pleistocene uplift of the dry valleys sector of the Transantarctic Mountains: a key parameter in ice-sheet reconstructions: Geology, v. 21, p. 841-844.

Wilch, T.I., McIntosh, W.C., Panter, K.S., Dunbar, N.W., Smellie, J.L., Fargo, A., Scanlan, M., Zimmerer, M.J., Ross, J., and Bosket, M.E., 2008, Volcanic and glacial geology of the Miocene Minna Bluff Volcanic Complex, Antarctica: [abstract] Eos (Transactions, American Geophysical Union), v. 89, Fall Meeting Supplement, abs.V11F–06.

Wilch, T.I., Panter, K.S., McIntosh, W.C., Dunbar, N.W., Smellie, J.L., Fargo, A., Ross, J., Antibus, J., Scanlan, M., Zimmerer, M., 2011. Miocene evolution of the Minna Bluff Volcanic Complex, Ross Embayment, Antarctica. International Symposium on Antarctic Earth Science XI, Edinburgh, Scotland, July 10-15. Abstract PS5.10.

Wright, A.C., and Kyle, P.R., 1990a, Mt. Bird, *in* LeMasurier, W.E., and Thomson, J.W., eds., Volcanoes of the Antarctic plate and southern oceans: American Geophysical Union Antarctic Research Series, v. 48, p. 97–98.

Wright, A.C., and Kyle, P.R., 1990b, Mt. Terror, *in* LeMasurier, W.E., and Thomson, J.W., eds., Volcanoes of the Antarctic plate and southern oceans: American Geophysical Union Antarctic Research Series, v. 48, p. 99–102.

Wright, A.C., and Kyle P.R., 1990c, Mount Morning, *in* LeMasurier, W.E., and Thomson, J.W., eds., Volcanoes of the Antarctic plate and southern oceans: American Geophysical Union Antarctic Research Series, v. 48, p. 124–126.

Wright, A.C., and Kyle P.R., 1990d, Mason Spur, *in* LeMasurier, W.E., and Thomson, J.W., eds., Volcanoes of the Antarctic plate and southern oceans: American Geophysical Union Antarctic Research Series, v. 48, p. 128–130.

Wright-Grassham, A.C., 1987, Volcanic geology, mineralogy and petrogenesis of the Discovery volcanic subprovince, southern Victoria Land, Antarctica [Ph.D. Thesis]: New Mexico Institute of Mining and technology. 460 pp. Unpublished.

Zachos, J.C., Dickens, G.R., and Zeebe, R.E., 2008, An early Cenozoic perspective on greenhouse warming and carbon-cycle dynamics: Nature, v. 451, p. 279-283.

Figures

Figure 1. Map of southern Victoria Land, Antarctica, showing the location of AND-2A Southern McMurdo Sound (SMS) core site and relevant geological features of Erebus Volcanic Province. Map also shows outcrops of volcanic rocks (in dark brown) belonging to the McMurdo Volcanic Group with relative time span of activity according to K-Ar and ^{40}Ar-^{39}Ar ages (Mercer, 1968; Kyle and Cole, 1974; Mayewski, 1975; Armstrong, 1978; Kyle, 1981, 1982, and 1990a,b; Kyle and Muncy, 1989; Wright and Kyle, 1990a, b; McKelvey et al., 1991; Wilch et al., 1993; Marchant et al., 1996; Esser et al., 2004; Tauxe et al. 2004; Timms, 2006; Cooper et al., 2007; Lewis et al., 2007; Wilch et al., 2008; Paulsen and Wilson, 2009; Martin et al., 2010).

Figure 2. Core (left column) and thin section optical microscope images (right column) representative of the four main volcaniclastic sediment types identified in AND-2A core: A and A_1)

pyroclastic fall deposit (640.13 m b.s.f), B and B_1) resedimented pumice- and scoria-rich sandstone to lapillistone (709.13 m b.s.f.), C and C_1) resedimented, strongly laminated, ash-rich mudstone to sandstone (636.23 m b.s.f.) and D and D_1) shard-rich mudstones and sandstones (712.04 m b.s.f.). Dg = dense glass; lf = lava fragment; p = pumice; san = sanidine; sd = sideromelane.

Figure 3. Scanning electron microscope backscattered images representative of the four main volcaniclastic sediment types identified in AND-2A core: A) pyroclastic fall deposit (dg = dense glass; p = pumice), B) resedimented pumice- and scoria-rich sandstone to lapillistone, C) resedimented, strongly laminated, ash-rich mudstone to sandstone and D) shard-rich mudstones and sandstones. Bio = bioclast; dg = dense glass; lf = lava fragment; p = pumice; qz = quartz; san = sanidine; sd = sideromelane. E) rims of leached glass occurring at the surface of the grains, along fractures and vesicles; F) pervasive perlitic fractures occurring chiefly in glass shards and in the least vesicular fragments.

Figure 4. AI–CCPI "Alteration box plot" diagram from Large et al. (2001) for analyzed AND-2A glass fragments. Data show different degrees and styles of alteration within studied samples. Colored rectangles identify least altered 'boxes' for unaltered rocks with <52 wt.% SiO_2, 52-63 wt.% SiO_2, 63-69 wt.% SiO_2 and >69 wt.% SiO_2, respectively. Full and open symbols respectively represent the composition of unaltered glass and altered glass within the same sample.

Figure 5. Total Alkali versus Silica diagrams (TAS) from LeMaitre (1989) for unaltered AND-2A glass compositions (blue diamonds). For comparison between composition of glasses in AND-2A and Erebus volcanic province products (red dashed curve; Armienti et al., 1998 and references therein), glass composition of fragment recovered in CRP1 (black crosses), 2/2A (black open squares; Armienti et al., 1998; Armienti et al., 2001), volcanic products of the Phase I activity of Mt. Morning (black open circles; Martin et al., 2010) and Mt. Morning volcanic rocks (pale red open squares; Muncy, 1979; Wright-Grassham, 1987; Martin et al., 2010) are also reported.

Figure 6. Harker's diagrams for unaltered AND-2A glass shards (blue diamonds). Glass compositions are compared with the compositions of glass fragments recovered in CRP1 (black crosses), 2/2a drillcores (black open squares) and attributed to proto-Mt. Morning and Mt. Morning activity (Armienti et al., 1998; Armienti et al., 2001). Whole rock composition of Mt. Morning volcanic rocks (Muncy, 1979; Wright-Grassham, 1987; Martin et al., 2010) are also reported (pale red open squares)

Figure 7. SiO_2 vs. sample depth diagram. The diagram indicates a general correlation between depth and the SiO_2 content of glasses (reconstructed compositions): altered rhyolitic-trachytic compositions occur prevalently above 709.19 m b.s.f. whereas sample at 831.68 m b.s.f marks the passage towards rhyolitic glass compositions occurring between 953.28 m b.s.f. and core base.

Figure 8. Schematic model illustrating possible eruptive, transport, and depositional processes of pyroclastic fall deposit, resedimented volcaniclastic deposits and the volcanogenic sedimentary deposits. A) pyroclasts transported by a high eruptive column and finally deposited as pyroclastic fall deposit directly through the water column in open water conditions; B) pumice and scoria clasts windblown over the ice and resedimented by suspension settling from ice-proximal turbid meltwater plumes or by low energy volcaniclastic bottom/turbidity currents (resedimented volcaniclastic deposits); C) volcanic detritus deposited by glaci-marine processes (volcanogenic sedimentary deposits).

Table 1. Descriptions of lithology and age data for pyroclastic fall deposit, resedimented volcaniclastic deposits and volcanogenic sedimentary deposits analyzed in AND-2A core.

Table 2. Major elements chemical composition of unaltered glasses within AND-2A core of pyroclastic fall deposit, resedimented volcaniclastic deposits and volcanogenic sedimentary deposits (expressed as oxides weight %). The maximum and minimum values of SiO_2 wt.% are reported for each sample. Chemical compositions of samples at 627.46-48 and 954.05-08 m b.s.f. were not reported since they are entirely formed by altered glass shards.

Figure 1
Click here to download high resolution image

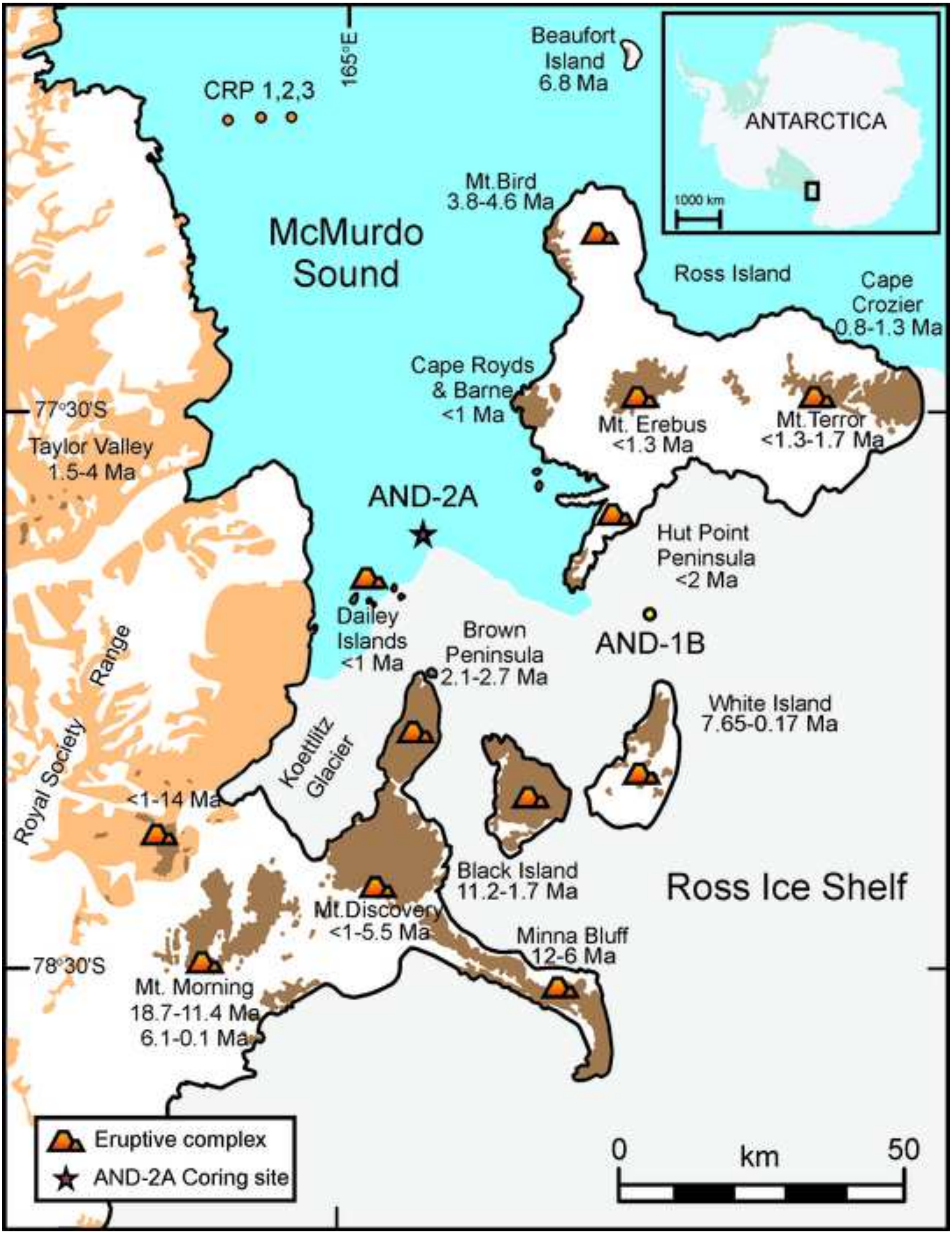

Figure 2

Click here to download high resolution image

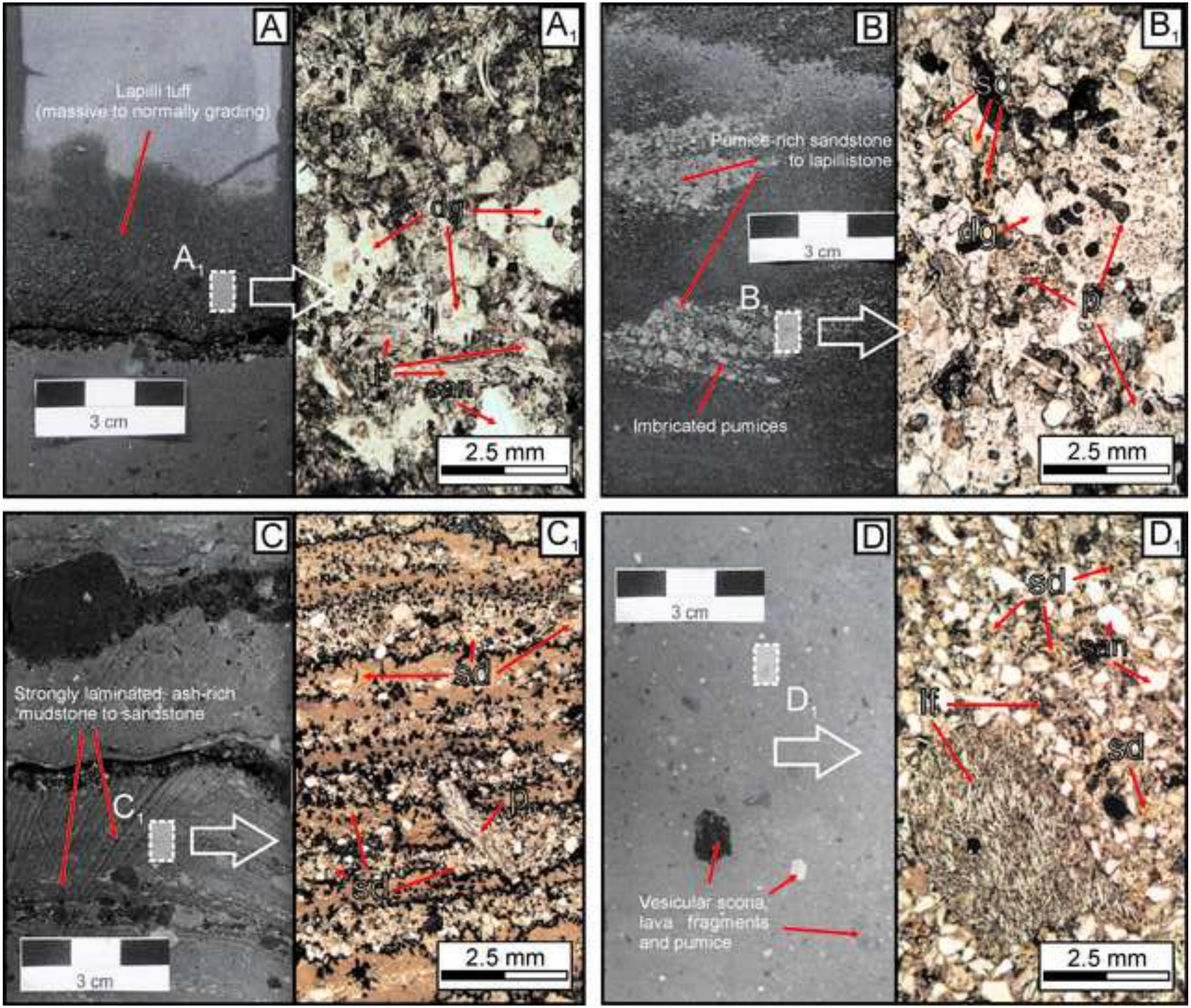

Figure 3
Click here to download high resolution image

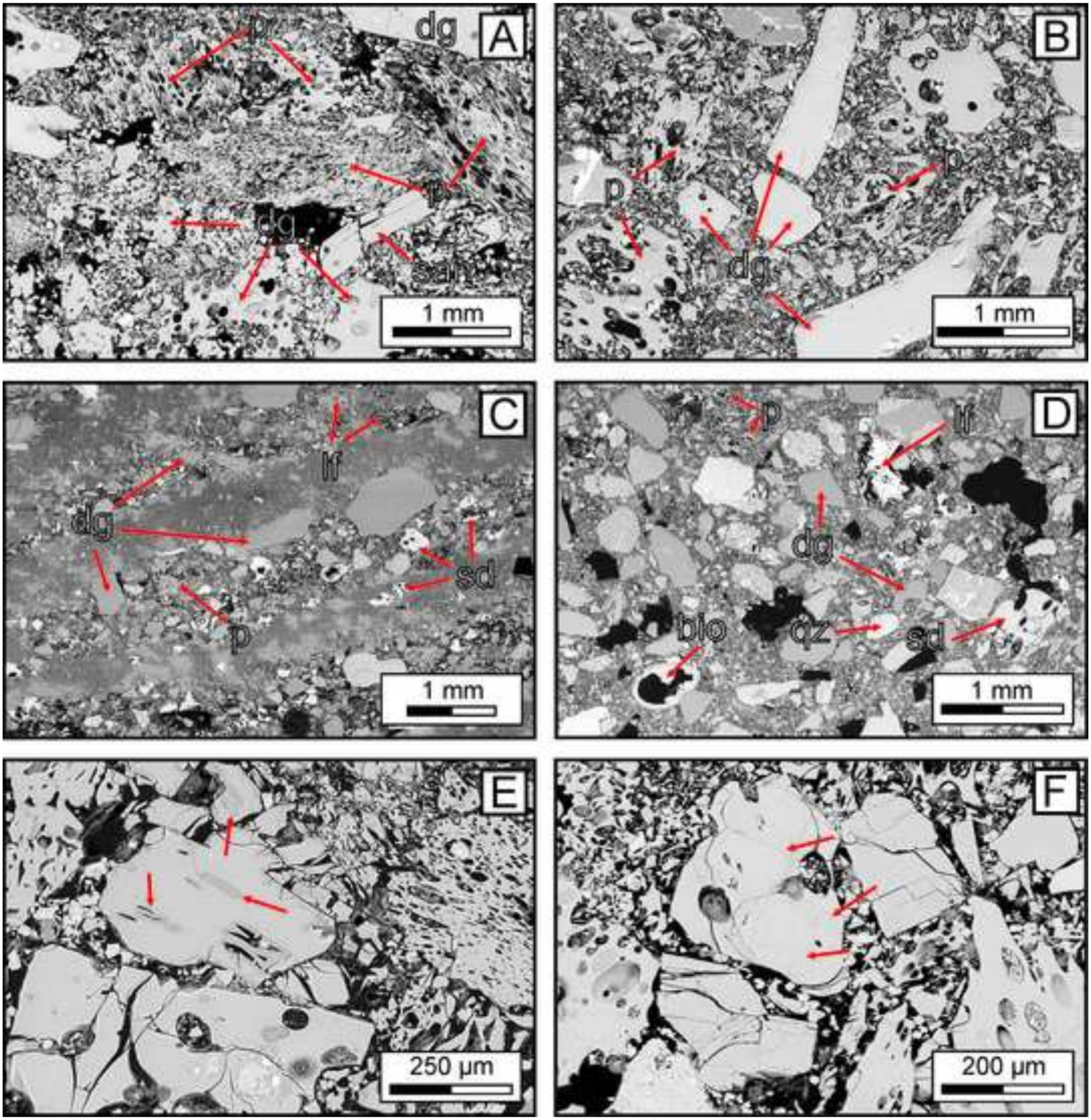

Figure 4

Click here to download high resolution image

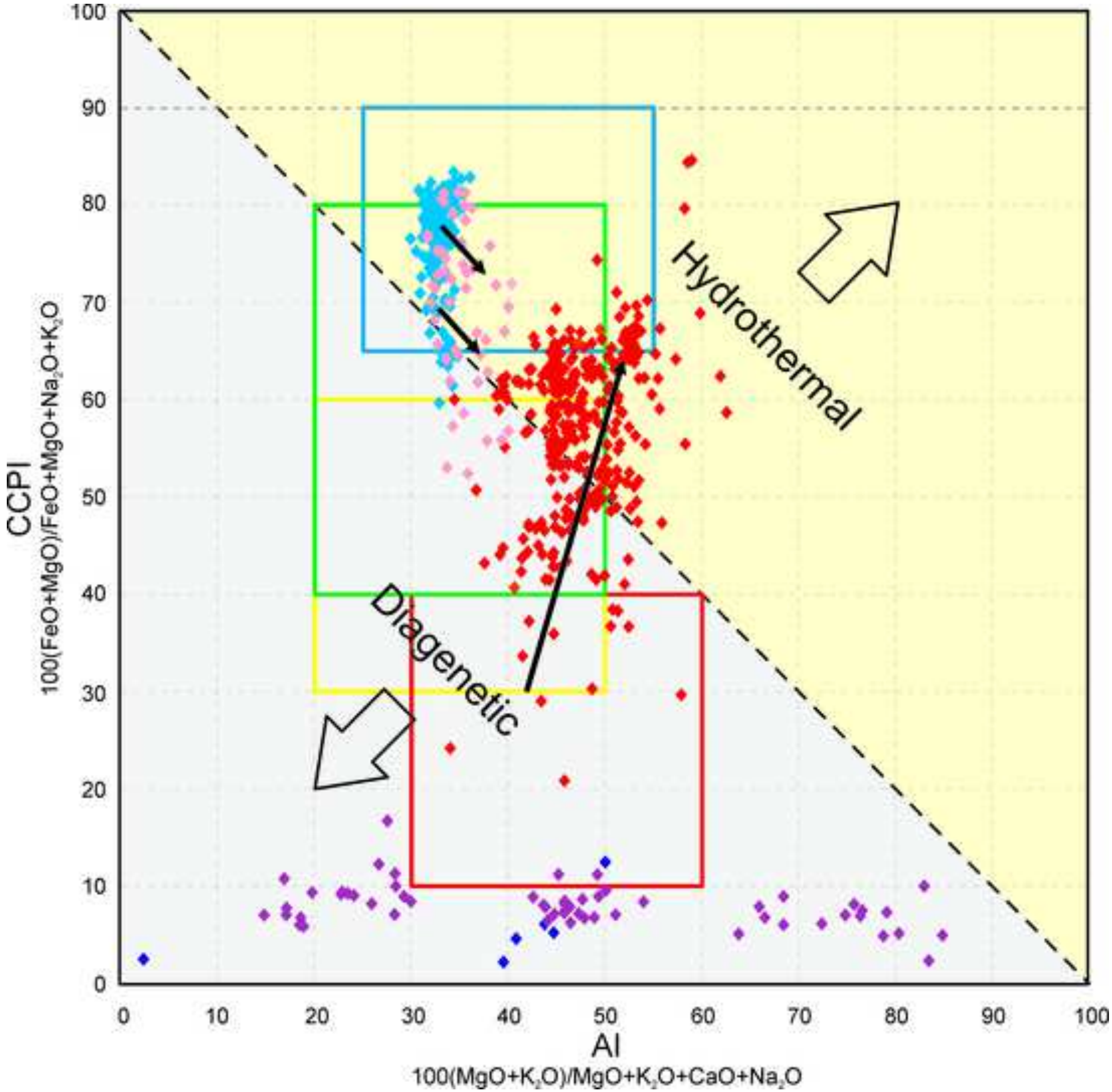

Figure 5

Click here to download high resolution image

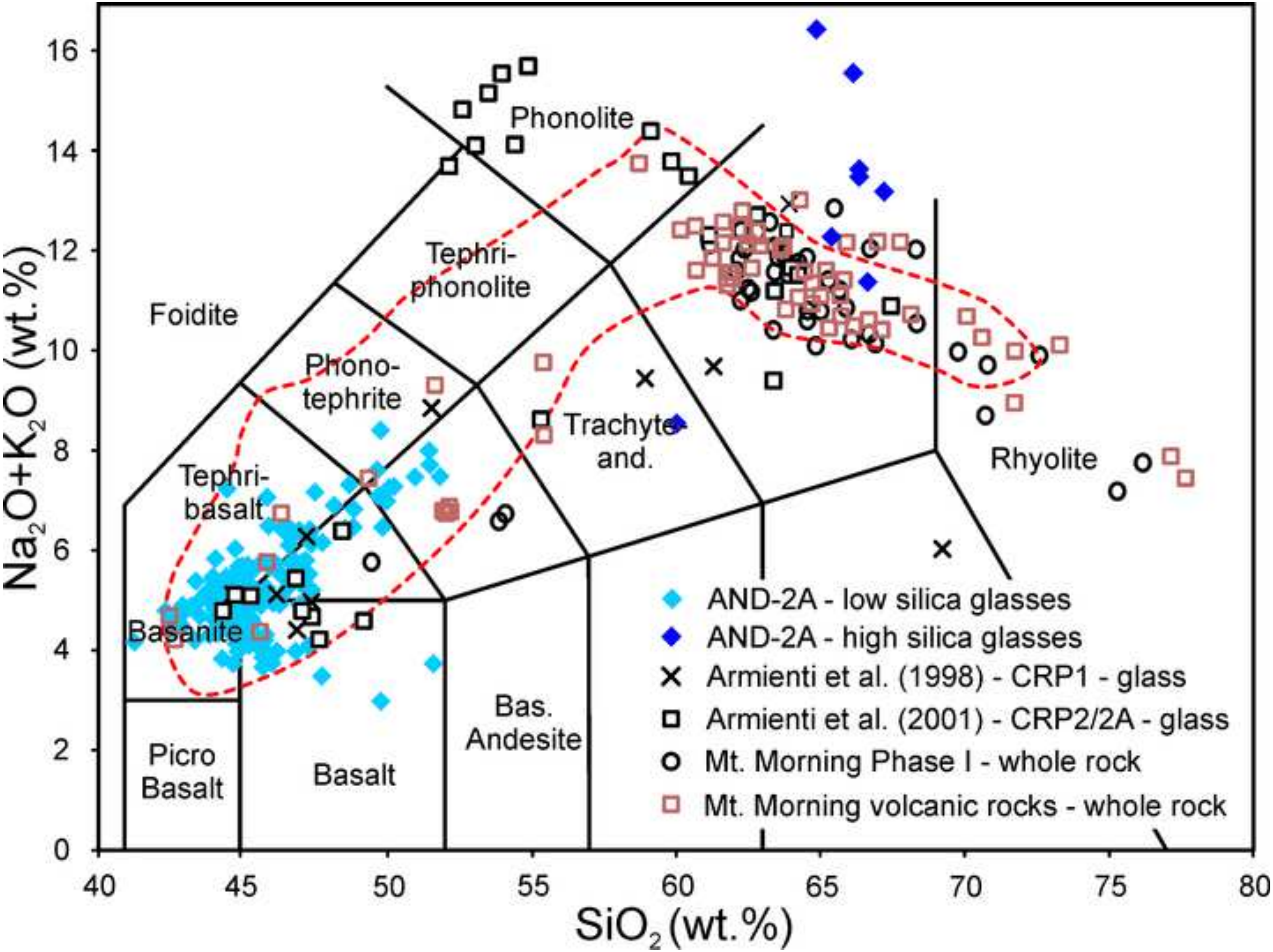

Figure 6
Click here to download high resolution image

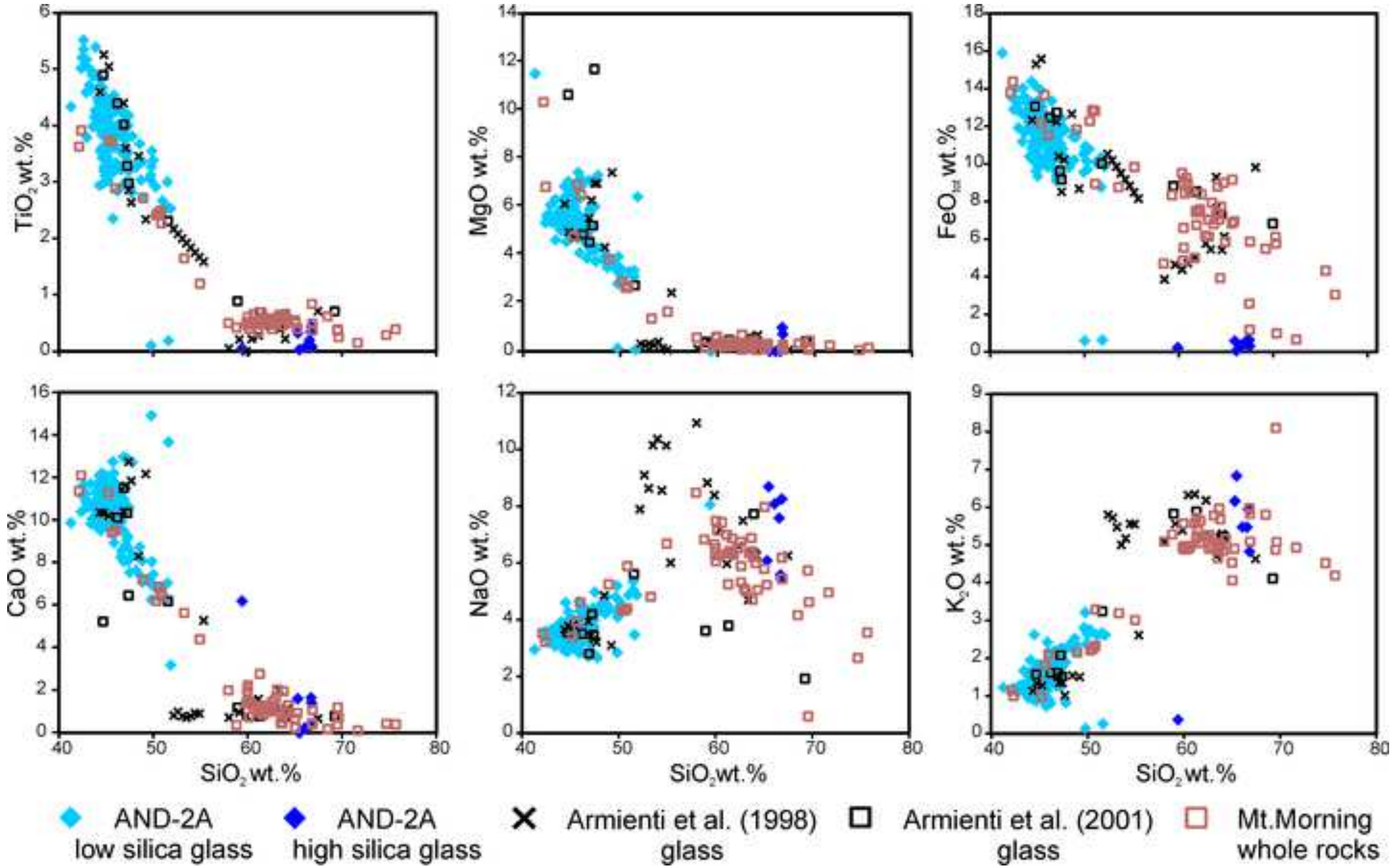

Figure 7
Click here to download high resolution image

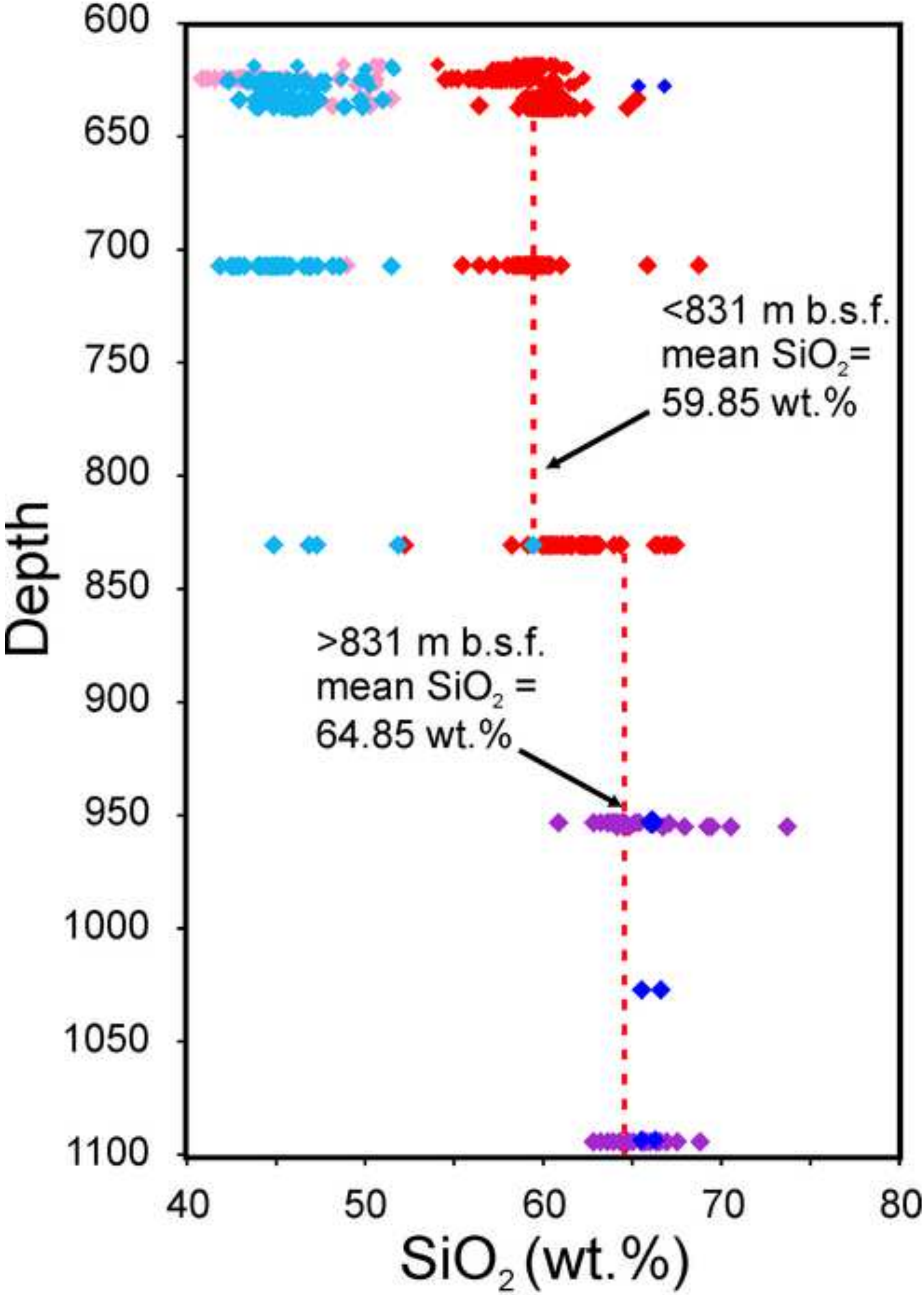

Figure 8
Click here to download high resolution image

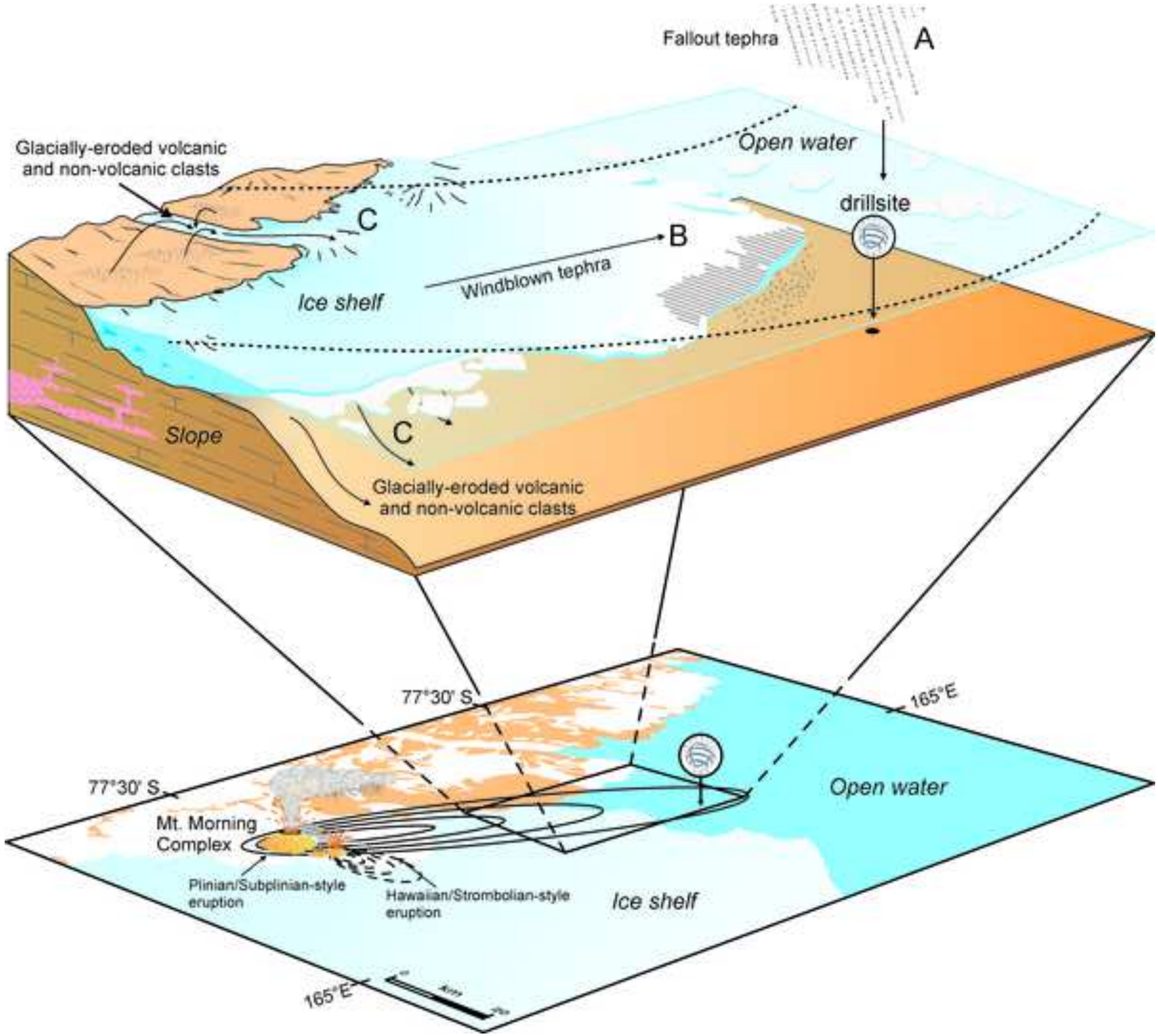

Table 1

TABLE 1. DESCRIPTION OF ANALYZED SAMPLES

Sample depth	LSU	Age (Ma)	Sediment type	Lithology	Glass composition (unaltered)
AND 2A - 621.24-27	LSU9	17.1-17.39	Resedimented volaniclastic	Resedimented pumice- and scoria-rich sandstone to lapillistone	Basanite/Mugearite
AND 2A - 622.65-67	LSU9	17.1-17.39	Volcanogenic	Shards-rich siltstone/sandstone	Basanite/Mugearite
AND 2A - 627.27-29	LSU9	17.1-17.39	Volcanogenic	Shards-rich siltstone/sandstone	Basalt/Basanite/Mugearite
AND 2A - 627.46-48	LSU9	17.1-17.39	Volcanogenic	Shards-rich siltstone/sandstone	N/A
AND 2A - 627.85-88	LSU9	17.1-17.39	Volcanogenic	Shards-rich siltstone/sandstone	Basanite/Basalt
AND 2A - 630.14-17	LSU9	17.1-17.39	Volcanogenic	Shards-rich siltstone/sandstone	Basanite/Mugearite
AND 2A - 636.20-22	LSU9	17.1-17.39	Resedimented volcaniclastic	Resedimented, laminated, ash-rich mudstone to sandstone	Basanite/Basalt
AND 2A - 636.23-26	LSU9	17.1-17.39	Resedimented volcaniclastic	Resedimented, laminated, ash-rich mudstone	Basanite/Mugearite
AND 2A - 639.27-30	LSU9	17.1-17.39	Volcanogenic	Shards-rich siltstone/sandstone	Basanite/Mugearite
AND 2A - 640.13-19	LSU9	17.39±0.12 $^{40}Ar/^{39}Ar$	Pyroclastic deposit	Lapilli tuff	Basanite
AND 2A - 709.14-16	LSU10	18.15±0.34 $^{40}Ar/^{39}Ar$	Resedimented volcaniclastic	Resedimented pumice- and scoria-rich sandstone to lapillistone	Basanite/Basalt
AND 2A - 709.17-19	LSU10	17.93±0.4 $^{40}Ar/^{39}Ar$	Resedimented volcaniclastic	Resedimented pumice- and scoria-rich sandstone to lapillistone	Basanite/Basalt
AND 2A - 709.19-21	LSU10	~17.39	Resedimented volcaniclastic	Resedimented pumice- and scoria-rich sandstone to lapillistone	Basanite/Basalt
AND 2A - 831.66-68	LSU11	18.71±0.33 $^{40}Ar/^{39}Ar$	Resedimented volcaniclastic	Resedimented pumice- and scoria-rich sandstone to lapillistone	Basanite/Basalt
AND 2A - 953.28-30	LSU12	19.44±0.34 $^{40}Ar/^{39}Ar$	Resedimented volcaniclastic	Resedimented pumice- and scoria-rich sandstone to lapillistone	Trachyte
AND 2A - 953.54-58	LSU12	19.49±0.34 $^{40}Ar/^{39}Ar$	Resedimented volcaniclastic	Resedimented pumice- and scoria-rich sandstone to lapillistone	Basanite
AND 2A - 954.05-08	LSU12	19.5-20	Resedimented volcaniclastic	Resedimented pumice- and scoria-rich sandstone to lapillistone	N/A
AND 2A - 1027.27-30	LSU13	19.5-20	Resedimented volcaniclastic	Resedimented, laminated, ash-rich mudstone to sandstone	Trachyte
AND 2A - 1093-03	LSU13	20.01±0.35 $^{40}Ar/^{39}Ar$	Resedimented volcaniclastic	Resedimented pumice- and scoria-rich sandstone to lapillistone	Trachyte

Note: Age are from Di Vincenzo et al. (2010); N/A - Not Available

Table 2

TABLE 2. CHEMICAL COMPOSITIONS OF ANALYZED VOLCANIC GLASS

Sample	621.24-22		636.20-22		636.23-26		640.13-19	709.14-16		709.17-19		709.19-21		831.66-68		953.28-30	953.56-58	1027.27-30		1093-03
SiO_2	43.80	51.50	42.96	46.38	43.86	50.99	46.11	42.86	48.19	42.49	51.48	42.63	48.58	44.90	59.42	66.83	41.29	49.81	66.56	66.24
TiO_2	4.16	3.01	3.80	3.24	4.27	2.67	4.27	5.07	3.27	5.21	2.56	5.52	3.68	4.00	0.05	0.08	4.34	0.10	0.19	0.04
Al_2O_3	15.25	15.35	14.86	16.24	14.83	15.78	15.09	14.55	15.67	13.51	15.88	13.19	13.73	15.93	24.24	18.17	11.73	30.84	18.09	18.55
FeO	12.49	10.34	11.92	10.15	12.85	10.09	12.33	12.91	10.82	12.89	8.76	13.97	11.45	10.02	0.23	0.31	15.90	0.60	0.61	0.87
MnO	0.14	0.27	0.19	0.21	0.18	0.15	0.24	0.23	0.23	0.24	0.25	0.28	0.32	0.26	0.00	0.00	0.25	0.00	0.01	0.05
MgO	5.61	3.36	5.38	4.81	5.54	3.31	5.13	5.62	3.84	5.59	3.11	5.68	4.01	5.86	0.00	0.71	9.87	0.12	0.03	0.03
CaO	10.87	7.04	10.93	10.23	10.89	6.81	9.87	11.26	7.62	11.15	6.29	11.65	8.73	11.78	6.19	0.44	11.51	14.91	0.33	0.13
Na_2O	3.82	5.04	3.49	4.36	3.83	4.86	4.07	3.43	4.53	3.47	5.35	3.38	4.22	3.77	8.06	8.25	2.95	2.84	7.59	7.56
K_2O	1.35	2.67	1.25	2.08	1.35	2.61	1.70	1.10	2.36	1.14	2.64	1.12	2.21	1.76	0.36	4.82	1.22	0.14	5.47	6.00
P_2O_5	1.50	1.09	1.56	1.19	1.38	1.18	0.99	1.61	1.42	1.63	1.11	1.65	1.39	0.77	0.00	0.02	0.00	0.01	0.00	0.01
Total	98.99	99.66	96.32	98.87	99.00	98.45	99.79	98.65	97.95	98.12	98.16	99.06	98.32	99.06	98.86	99.65	99.20	99.38	98.88	99.67
Alkali	5.17	7.71	4.74	6.44	5.18	7.47	5.77	4.53	6.90	4.61	7.99	4.51	6.43	5.53	8.42	13.08	4.16	2.98	13.05	13.56

Note: Values shown are the highest and lowest SiO_2 contents within a given sample

Supplemental file

Supplemental file

Click here to download Supplemental file: Suppl Figure 1.tif

Supplemental file
Click here to download Supplemental file: Suppl Table 1.tif